Published OnlineFirst January 11, 2013; DOI: 10.1158/1535-7163.MCT-12-0869

Molecular Cancer Therapeutics

Cancer Therapeutics Insights

Dual Programmed Cell Death Pathways Induced by p53 Transactivation Overcome Resistance to Oncolytic Adenovirus in Human Osteosarcoma Cells

Joe Hasei[1], Tsuyoshi Sasaki[1], Hiroshi Tazawa[2,4], Shuhei Osaki[1], Yasuaki Yamakawa[1], Toshiyuki Kunisada[1,3], Aki Yoshida[1], Yuuri Hashimoto[2], Teppei Onishi[2], Futoshi Uno[2], Shunsuke Kagawa[2], Yasuo Urata[5], Toshifumi Ozaki[1], and Toshiyoshi Fujiwara[2]

Abstract

Tumor suppressor p53 is a multifunctional transcription factor that regulates diverse cell fates, including apoptosis and autophagy in tumor biology. p53 overexpression enhances the antitumor activity of oncolytic adenoviruses; however, the molecular mechanism of this occurrence remains unclear. We previously developed a tumor-specific replication-competent oncolytic adenovirus, OBP-301, that kills human osteosarcoma cells, but some human osteosarcoma cells were OBP-301–resistant. In this study, we investigated the antitumor activity of a p53-expressing oncolytic adenovirus, OBP-702, and the molecular mechanism of the p53-mediated cell death pathway in OBP-301–resistant human osteosarcoma cells. The cytopathic activity of OBP-702 was examined in OBP-301–sensitive (U2OS and HOS) and OBP-301–resistant (SaOS-2 and MNNG/HOS) human osteosarcoma cells. The molecular mechanism in the OBP-702–mediated induction of two cell death pathways, apoptosis and autophagy, was investigated in OBP-301–resistant osteosarcoma cells. The antitumor effect of OBP-702 was further assessed using an orthotopic OBP-301–resistant MNNG/HOS osteosarcoma xenograft tumor model. OBP-702 suppressed the viability of OBP-301–sensitive and -resistant osteosarcoma cells more efficiently than OBP-301 or a replication-deficient p53-expressing adenovirus (Ad-p53). OBP-702 induced more profound apoptosis and autophagy when compared with OBP-301 or Ad-p53. E1A-mediated *miR-93/106b* upregulation induced p21 suppression, leading to p53-mediated apoptosis and autophagy in OBP-702–infected cells. p53 overexpression enhanced adenovirus-mediated autophagy through activation of damage-regulated autophagy modulator (DRAM). Moreover, OBP-702 suppressed tumor growth in an orthotopic OBP-301–resistant MNNG/HOS xenograft tumor model. These results suggest that OBP-702–mediated p53 transactivation is a promising antitumor strategy to induce dual apoptotic and autophagic cell death pathways via regulation of miRNA and DRAM in human osteosarcoma cells. *Mol Cancer Ther; 12(3); 314–25. ©2012 AACR.*

Introduction

Osteosarcoma is one of the most common malignant tumors in young children (1, 2). Current treatment strategies, which consist of multi-agent chemotherapy and aggressive surgery, have significantly improved the cure rate and prognosis of patients with osteosarcoma. In fact, over the past 30 years, the 5-year survival rate has increased from 10% to 70% (3–5). Even in patients with osteosarcoma with metastases at diagnosis, the 5-year survival rate has reached 20% to 30% in response to chemotherapy and surgical removal of primary and metastatic tumors (6). However, treatment outcomes for patients with osteosarcomas have further improved over the last few years. Therefore, the development of novel therapeutic strategies is required to improve the clinical outcomes in patients with osteosarcomas.

Tumor-specific replication-competent oncolytic viruses are being developed as novel anticancer therapy, in which the promoters of cancer-related genes are used to regulate virus replication in a tumor-dependent manner. More than 85% of all human cancers express high telomerase activity to maintain the length of the telomeres during cell division, whereas normal somatic cells seldom show this enhanced telomerase activity (7, 8). Telomerase activity has also been detected in 44% to 81% of bone and

Authors' Affiliations: Departments of [1]Orthopaedic Surgery, [2]Gastroenterological Surgery, and [3]Medical Materials for Musculoskeletal Reconstruction, Okayama University Graduate School of Medicine, Dentistry and Pharmaceutical Sciences; [4]Center for Innovative Clinical Medicine, Okayama University Hospital, Okayama; and [5]Oncolys BioPharma, Inc., Tokyo, Japan

Note: Supplementary data for this article are available at Molecular Cancer Therapeutics Online (http://mct.aacrjournals.org/).

Corresponding Author: Toshiyoshi Fujiwara, Department of Gastroenterological Surgery, Okayama University Graduate School of Medicine, Dentistry and Pharmaceutical Sciences, 2-5-1 Shikata-cho, Kita-ku, Okayama 700-8558, Japan. Phone: 81-86-235-7257; Fax: 81-86-221-8775; E-mail: toshi_f@md.okayama-u.ac.jp

doi: 10.1158/1535-7163.MCT-12-0869

Published OnlineFirst January 11, 2013; DOI: 10.1158/1535-7163.MCT-12-0869

soft-tissue sarcomas (9, 10). Telomerase activation is closely correlated with the expression of the human telomerase reverse transcriptase (*hTERT*) gene (11). On the basis of these data, we previously developed a telomerase-specific replication-competent oncolytic adenovirus OBP-301 (Telomelysin) in which the *hTERT* gene promoter drives the expression of the *E1A* and *E1B* genes (12). A phase I clinical trial of OBP-301, which was conducted in the United States on patients with advanced solid tumors, indicated that OBP-301 was well tolerated by patients (13). Recently, we reported that OBP-301 efficiently killed human bone and soft-tissue sarcoma cells (14, 15). However, some osteosarcoma cell lines were not sensitive to the antitumor effect of OBP-301. Therefore, to efficiently eliminate tumor cells with OBP-301, its antitumor effects need to be enhanced.

Cancer gene therapy is defined as the treatment of malignant tumors via the introduction of a therapeutic tumor suppressor gene or the abrogation of an oncogene. The tumor suppressor *p53* gene has an attractive tumor suppressor profile as a potent therapeutic transgene for induction of cell-cycle arrest, senescence, apoptosis, and autophagy (16). Dual cell death pathways, such as apoptosis and autophagy, induced by p53 transactivation are mainly involved in the suppression of tumor initiation and progression. However, among the p53 downstream target genes, p21, which is most rapidly and strongly induced during the DNA damage response, mainly induces cell-cycle arrest through suppression of apoptotic and autophagic cell death pathways (17, 18). Thus, p21 suppression may be a more effective strategy for the induction of apoptotic and autophagic cell death pathways in tumor cells, particularly when the tumor suppressor *p53* gene is overexpressed in tumor cells in response to cancer gene therapy.

A p53-expressing replication-deficient adenovirus (Ad-p53, Advexin) has previously been reported to induce an antitumor effect in the *in vitro* and *in vivo* settings (19, 20) as well as in some clinical studies (21–24). We recently reported that combination therapy with OBP-301 and Ad-p53 resulted in a more profound antitumor effect than monotherapy with either OBP-301 or Ad-p53 (25). Moreover, we generated armed OBP-301 expressing the wild-type *p53* tumor suppressor gene (OBP-702) and showed that OBP-702 suppressed the viability of various types of epithelial malignant cells more efficiently than did OBP-301 (26). OBP-702 induced a more profound apoptotic cell death effect than Ad-p53, likely via adenoviral E1A-mediated suppression of anti-apoptotic p21 in human epithelial malignant cells. However, it remained unclear whether OBP-702 efficiently induces an antitumor effect in human nonepithelial malignant cells, including osteosarcomas.

In the present study, we investigated the *in vitro* cytopathic efficacy of the p53-expressing telomerase-specific replication-competent oncolytic adenovirus, OBP-702, in human osteosarcoma cells, and we compared the induction level of apoptotic and autophagic cell deaths in OBP-301–resistant human osteosarcoma cells infected with OBP-301, OBP-702, and Ad-p53. The molecular mechanism by which OBP-702 mediates induction of apoptosis and autophagy was also investigated. Finally, the *in vivo* antitumor effect of OBP-702 was evaluated using an orthotopic OBP-301–resistant human osteosarcoma xenograft tumor model.

Materials and Methods

Cell lines

The human osteosarcoma cell lines, HOS and SaOS-2, were kindly provided by Dr. Satoru Kyo (Kanazawa University, Ishikawa, Japan). These cells were propagated as monolayer cultures in Dulbecco's Modified Eagle's Medium. The human osteosarcoma cell line, U2OS, was obtained from the American Type Culture Collection and was grown in McCoy's 5a Medium. The human osteosarcoma cell line, MNNG/HOS, was purchased from DS Pharma Biomedical and was maintained in Eagle's Minimum Essential Medium containing 1% nonessential amino acids. All media were supplemented with 10% FBS, 100 U/mL penicillin, and 100 mg/mL streptomycin. The normal human lung fibroblast (NHLF) cell line, NHLF, was obtained from TaKaRa Biomedicals. NHLF cells were propagated as monolayer culture in the medium recommended by the manufacturer. Although cell lines were not authenticated by the authors, cells were immediately expanded after receipt and stored in liquid N_2. Cells were not cultured for more than 5 months following resuscitation. The cells were maintained at 37°C in a humidified atmosphere with 5% CO_2.

Recombinant adenoviruses

The recombinant telomerase-specific replication-competent adenovirus OBP-301 (Telomelysin), in which the promoter element of the *hTERT* gene drives the expression of *E1A* and *E1B* genes, was previously constructed and characterized (12, 27). For OBP-301–mediated induction of exogenous *p53* gene expression, we recently generated OBP-702, in which a human wild-type *p53* gene expression cassette was inserted into the *E3* region (Supplementary Fig. S1; ref. 26). Ad-p53 is a replication-defective adenovirus serotype 5 vector with a *p53* gene expression cassette at the *E1* region (19, 20). Recombinant viruses were purified by ultracentrifugation using cesium chloride step gradients, their titers were determined by a plaque-forming assay using 293 cells and they were stored at −80°C.

Cell viability assay

Cells were seeded on 96-well plates at a density of 1×10^3 cells/well 24 hours before viral infection. All cell lines were infected with OBP-702 at multiplicity of infections (MOI) of 0, 0.1, 1, 10, 50, or 100 plaque-forming units (PFU)/cell. Cell viability was determined on days 1, 2, 3, and 5 after virus infection using Cell Proliferation Kit II (Roche Molecular Biochemicals). The 50% inhibiting dose (ID_{50}) value of OBP-702 for each cell line was calculated

Published OnlineFirst January 11, 2013; DOI: 10.1158/1535-7163.MCT-12-0869

using cell viability data obtained on day 5 after virus infection.

Time-lapse confocal laser microscopy

GFP-expressing MNNG/HOS (MNNG/HOS-GFP) cells were established by stable transfection with GFP expression plasmid using Lipofectamine LTX (Invitrogen). MNNG/HOS-GFP and NHLF cells were seeded in 35-mm glass-based dishes at a density of 1×10^5 cells/dish 24 hours before infection and were infected with OBP-702 at an MOI of 10 PFU/cell for 72 hours. Phase-contrast and fluorescence time-lapse recordings were obtained to concomitantly analyze cell morphology and GFP expression using an inverted FV10i confocal laser scanning microscopy (OLYMPUS).

Western blot analysis

SaOS-2 and MNNG/HOS cells, seeded in a 100-mm dish at a density of 1×10^5 cells/dish, were infected with OBP-301, OBP-702, or Ad-p53 at the indicated MOIs. In contrast, SaOS-2 cells were transfected with 10 nmol/L *miR-93* (Ambion), *miR-106b* (Ambion), or control miRNA (Ambion) 24 hours before Ad-p53 infection and infected with Ad-p53 at an MOI of 100 for 48 hours. Whole-cell lysates were prepared in a lysis buffer [50 mmol/L Tris-HCl (pH 7.4), 150 mmol/L NaCl, 1% Triton X-100] containing a protease inhibitor cocktail (Complete Mini; Roche) at the indicated time points. Proteins were electrophoresed on 6% to 15% SDS-PAGE and were transferred to polyvinylidene difluoride membranes (Hybond-P; GE Health Care). Blots were blocked with 5% non-fat dry milk in TBS-T (Tris-buffered saline and 0.1% Tween-20, pH 7.4). The primary antibodies used were: rabbit anti-PARP polyclonal antibody (pAb; Cell Signaling Technology), mouse anti-p53 monoclonal antibody (mAb; Calbiochem), mouse anti-$p21^{WAF1}$ mAb (Calbiochem), rabbit anti-E2F1 pAb (Santa Cruz Biotechnology), mouse anti-Ad5 E1A mAb (BD PharMingen), rabbit anti-microtubule-associated protein 1 light chain 3 (LC3) pAb [Medical & Biological Laboratories (MBL)], mouse anti-p62 mAb (MBL), rabbit anti-damage-regulated autophagy modulator (DRAM) pAb (Abgent), and mouse anti-β-actin mAb (Sigma-Aldrich).

Flow cytometric analysis

To analyze the active caspase-3 expression, cells were incubated for 20 minutes on ice in Cytofix/Cytoperm solution (BD Biosciences), labeled with phycoerythrin (PE)-conjugated rabbit anti-active caspase-3 mAb (BD Biosciences) for 30 minutes, and then analyzed using FACS array (BD Biosciences).

To evaluate the sub-G_1 population, which is a apoptosis indicator, in SaOS-2 cells after virus infection, SaOS-2 cells were seeded in a 100-mm dish at a density of 1×10^6 cells/dish 24 hours before viral infection and were infected with mock, OBP-301, Ad-p53, or OBP-702 at an MOI of 10 PFUs/cell for 48 hours. Cells were trypsinized and resuspended in original supernatant to ensure that both attached and nonattached cells were analyzed. Cells stained with propidium iodide were analyzed using FACS array (BD Biosciences).

Quantitative real-time reverse transcription PCR analysis

To evaluate the expressions of *miR-93* and *miR-106b* in tumor cells after OBP-702 infection, SaOS-2 and MNNG/HOS cells were seeded on 6-well plates at a density of 2×10^5 cells/well 24 hours before viral infection and were infected with OBP-702 at MOIs of 0, 1, 5, 10, 50, or 100 PFU/cell. Three days after virus infection, total RNA was extracted from the cells using a miRNeasy Mini Kit (Qiagen). The concentration and quality of RNA were assessed using a Nanodrop spectrophotometer. cDNA was synthesized from 10 ng of total RNA using the TaqMan MicroRNA Reverse Transcription Kit (Applied Biosystems), and quantitative real-time reverse transcription (RT)-PCR was carried out using the Applied Biosystems StepOnePlus real-time PCR System. The expressions of *miR-93* and *miR-106b* were defined from the threshold cycle (C_t), and relative expression levels were calculated using the $2^{-\Delta\Delta C_t}$ method after normalization with reference to the expression of U6 small nuclear RNA.

***In vivo* orthotopic MNNG/HOS xenograft tumor model**

Animal experimental protocols were approved by the Ethics Review Committee for Animal Experimentation of Okayama University School of Medicine (Okayama, Japan). MNNG/HOS cells (5×10^6 cells per site) were inoculated into the tibias of female athymic nude mice aged 6 to 7 weeks (CLEA Japan). Palpable tumors developed within 21 days and were permitted to grow to approximately 5 to 6 mm in diameter. At that stage, a 50-μL volume of solution containing OBP-702, OBP-301, or Ad-p53 at a dose of 1×10^8 PFU or PBS was injected into the tumors for 3 cycles every 2 days. Tumor volume was monitored by computed tomographic (CT) imaging once a week after virus infection.

Three-dimensional computed tomography imaging

The tumor volume and formation of osteolytic lesions were evaluated using three-dimensional CT (3D-CT) imaging (ALOKA Latheta LCT-200; Hitachi Aloka Medical). The tumor volume was calculated by INTAGE Realia software (Cybernet Systems).

Histopathologic analysis

Tumors were fixed in 10% neutralized formalin and embedded in paraffin blocks. Sections were stained with hematoxylin/eosin and analyzed by light microscopy.

Statistical analysis

Data are expressed as means ± SD. Student *t* test was used to compare differences between groups. Statistical significance was defined as $P < 0.05$.

Published OnlineFirst January 11, 2013; DOI: 10.1158/1535-7163.MCT-12-0869

Results

In vitro cytopathic efficacy of OBP-702 against human osteosarcoma cell lines

To evaluate the *in vitro* cytopathic activity of OBP-702, we used the 2 OBP-301–sensitive human osteosarcoma cells (HOS and U2OS) and the 2 OBP-301–resistant human osteosarcoma cells (SaOS-2 and MNNG/HOS) that were recently described (14). The cell viability of each cell was assessed over 5 days after infection using the XTT assay. OBP-702 infection suppressed the viability of OBP-301–sensitive and -resistant cells in dose- and time-dependent manners (Fig. 1A and B). When the ID_{50} values of OBP-702 in all 4 human osteosarcoma cells were compared with those of OBP-301 calculated in a previous report (14), all cell lines were more sensitive to OBP-702 than to OBP-301 (Table 1). The ID_{50} values of OBP-702 were also lower than those of Ad-p53 (Supplementary Fig. S2). However, OBP-702 did not exhibit any cytopathic effect in NHLF cells (Fig. 1B). When GFP-expressing MNNG/HOS-GFP cells were cocultured with human normal NHLF cells, OBP-702 infection showed a cytopathic effect (confirmed by observation of round-shaped morphologic changes) in MNNG/HOS-GFP cells but not in NHLF cells (Fig. 1C). These results indicate that OBP-702 was more cytopathic than OBP-301 for human osteosarcoma cells but was not cytopathic for normal human cells.

Increased induction of apoptosis by OBP-702 when compared with OBP-301 or Ad-p53

We next investigated whether OBP-702 induces more profound apoptosis when compared with OBP-301 or Ad-p53. OBP-301–resistant SaOS-2 and MNNG/HOS cells

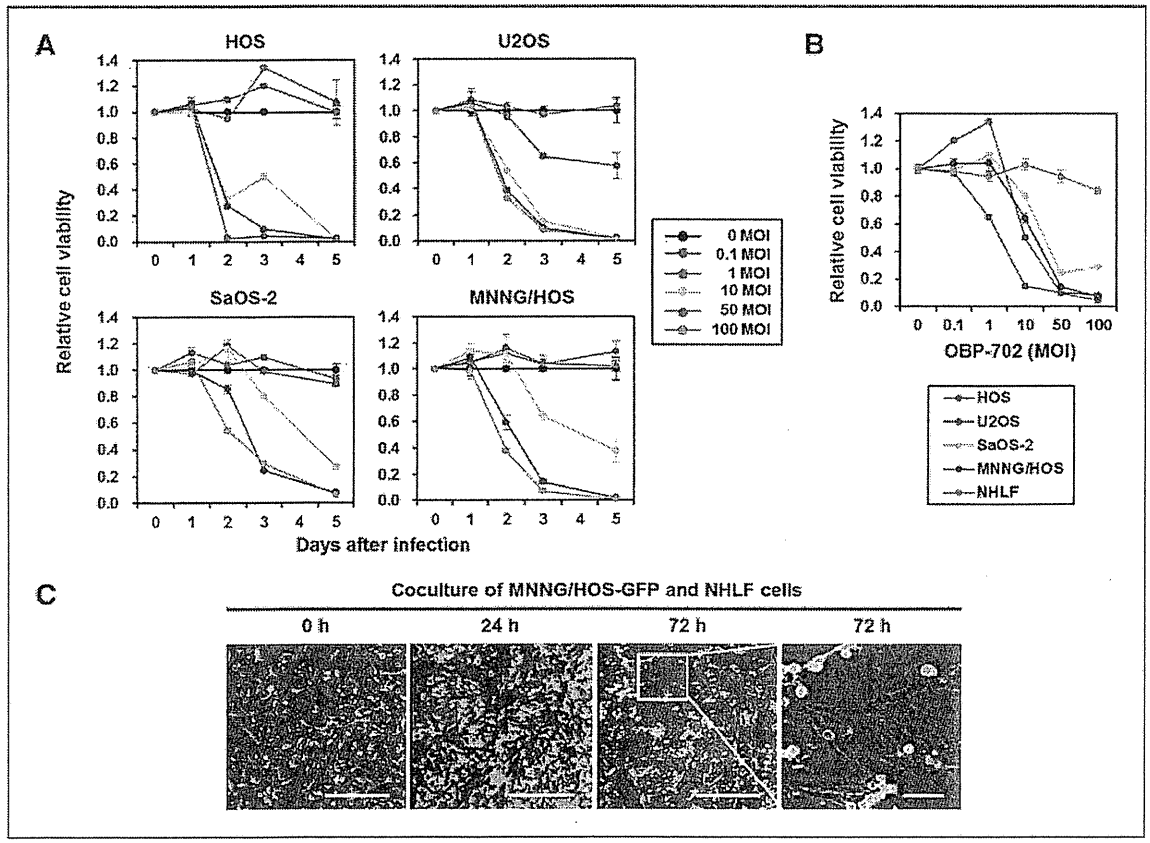

Figure 1. *In vitro* cytopathic effect of OBP-702 in human osteosarcoma cell lines. A, OBP-301–sensitive (HOS and U2OS) and OBP-301–resistant (SaOS-2 and MNNG/HOS) human osteosarcoma cells were infected with OBP-702 at the indicated MOI, and cell viability was quantified over 5 days using the XTT assay. Cell viability was calculated relative to that of the mock-infected group on each day, which was set at 1.0. Cell viability data are expressed as mean values ± SD ($n = 5$). B, four human osteosarcoma cells and one normal fibroblast NHLF cell were seeded 24 hours before viral infection and were infected with OBP-702 at the indicated MOIs, and cell viability was examined on day 5 using the XTT assay. Cell viability was calculated relative to that of the mock-infected group, which was set at 1.0. Cell viability data are expressed as mean ± SD ($n = 5$). C, time lapse images of cytopathic effect of OBP-702 in coculture of GFP-expressing MNNG/HOS cells with human normal fibroblast NHLF cells. MNNG/HOS-GFP cells coincubated with NHLF cells were recorded for 72 hours after OBP-702 infection at an MOI of 10. Three images on the left are low magnification and one image on the right is high magnification of the area outlined by a white square. Left scale bars, 100 μm. Right scale bar, 10 μm.

Published OnlineFirst January 11, 2013; DOI: 10.1158/1535-7163.MCT-12-0869

Table 1. Comparison of ID_{50} values of OBP-301 and OBP-702 in various human osteosarcoma cell lines

Cell lines	Sensitivity to OBP-301	Cell type	Relative hTERT mRNA expression	ID_{50} value[a] (MOI)		Ratio[b] (OBP-702/ OBP-301)
				OBP-301	OBP-702	
SaOS-2	Resistant	ALT	Negative	98.1	5.5	0.06
MNNG/HOS	Resistant	Non-ALT	1	97.3	6.7	0.07
U2OS	Sensitive	ALT	0.3	38.2	1.2	0.03
HOS	Sensitive	Non-ALT	4.3	43.0	4.5	0.10

[a]The ID_{50} values of OBP-702 and OBP-301 were calculated from the data of XTT assay on day 5 after infection.
[b]The ratio was calculated from the division of the ID_{50} value of OBP-702 by the ID_{50} value of OBP-301.

were infected with OBP-702, OBP-301, or Ad-p53, and apoptosis was assessed by Western blot and flow cytometric analyses. Western blot analysis showed that SaOS-2 cells exhibited the cleavage of PARP after infection with OBP-702 (>5 MOIs) or Ad-p53 (>50 MOIs), whereas MNNG/HOS cells had the cleavage of PARP after infection with OBP-702 (>5 MOIs) but not Ad-p53 (Fig. 2A). In contrast, OBP-301 did not induce apoptosis (data not shown). Furthermore, flow cytometric analysis showed that OBP-702 infection (10 MOIs) significantly increased the percentage of apoptotic cells with active caspase-3 when compared with Ad-p53 or OBP-301 at same doses in SaOS-2 and MNNG/HOS cells (Fig. 2B and C). Cell-cycle analysis also showed that OBP-702 (10 MOIs) induced the highest percentages of sub-G_1 population in SaOS-2 cells when compared with Ad-p53 or OBP-301 at same doses (Fig. 2D). These results suggest that OBP-702 induces increased apoptosis when compared with Ad-p53 or OBP-301 in human osteosarcoma cells.

p53 induction in human osteosarcoma cells infected with OBP-702

To investigate the molecular mechanism of OBP-702–induced apoptosis in human osteosarcoma cells, we evaluated p53 expression after OBP-702 infection in SaOS-2 (p53-null) and MNNG/HOS (p53-mutant) cells in which endogenous p53 expression level was confirmed by Western blot analysis (Supplementary Fig. S3). OBP-702 efficiently induced p53 expression in SaOS-2 and MNNG/HOS cells (Fig. 3A). The level of p53 expression was higher in OBP-702–treated cells than in Ad-p53–treated cells (Fig. 3A). Despite of OBP-702–induced high p53 expression, p53 downstream target p21 protein was induced only in Ad-p53–treated cells.

To investigate the effect of exogenous p53 overexpression in virus replication, we next compared the replication abilities of OBP-702 and OBP-301 in p53-null SaOS-2 cells by measuring the relative amounts of *E1A* copy numbers. The *E1A* copy number of OBP-702 was similar to that of OBP-301 in SaOS-2 cells (Supplementary Fig. S4). These results indicate that OBP-702 efficiently induces exogenous p53 expression without affecting p21 expression and virus replication in human osteosarcoma cells.

OBP-702–mediated upregulation of *miR-93* and *miR-106b* suppresses p21 expression

Adenoviral E1A protein has been shown to activate E2F1 expression (28), which is a multifunctional transcription factor that regulates diverse cell fates through induction of many target genes, including small noncoding miRNAs (29). Recently, E2F1-inducible *miR-93* and *miR-106b* have been shown to suppress p21 expression in human cancer cells (30). Therefore, we sought to investigate whether OBP-702 induces expressions of E2F1 and E2F1-regulated miRNAs (*miR-93* and *miR-106b*). OBP-702 infection activated E2F1 expression along with E1A accumulation in SaOS-2 and MNNG/HOS cells (Fig. 3B). The expression levels of *miR-93* and *miR-106b* were increased in association with E2F1 activation in OBP-702–infected SaOS-2 and MNNG/HOS cells (Fig. 3C). In contrast, E1A-deleted Ad-p53 infection did not increase expressions of E2F1 and E2F1-regulated *miR-93* and *miR-106b* (data not shown). Next, we assessed whether upregulation of *miR-93* and *miR-106b* efficiently suppresses p21 expression induced by Ad-p53–mediated p53 overexpression. Ad-p53 infection at MOIs of 10 and 100 efficiently induced p21 expression at 48 hours after infection in SaOS-2 cells (Supplementary Fig. S5). When SaOS-2 cells were infected with Ad-p53 at an MOI of 100 for 48 hours, pretransfection with *miR-93*, *miR-106b*, or both efficiently suppressed Ad-p53–induced p21 expression (Fig. 3D). Interestingly, both *miR-93*- and *miR-106b*–transfected SaOS-2 cells showed the 1.5-fold increased expression of cleaved PARP (C-PARP) in consistency with remarkable p21 downregulation when compared with those transfected with control miR. However, the expression level of C-PARP was not increased in the *miR-93*- or *miR-106b*–transfected SaOS-2 cells, although transfection with *miR-93* or *miR-106b* moderately decreased p21 expression. These results suggest that OBP-702 suppresses p21 expression through E1A-dependent upregulation of both E2F1-inducible *miR-93* and *miR-106b* and contributes to induction of apoptosis.

Increased induction of autophagy by OBP-702 when compared with OBP-301

Recently, we showed that oncolytic adenovirus OBP-301 mainly induces programmed cell death in association with autophagy rather than apoptosis in human tumor

Published OnlineFirst January 11, 2013; DOI: 10.1158/1535-7163.MCT-12-0869

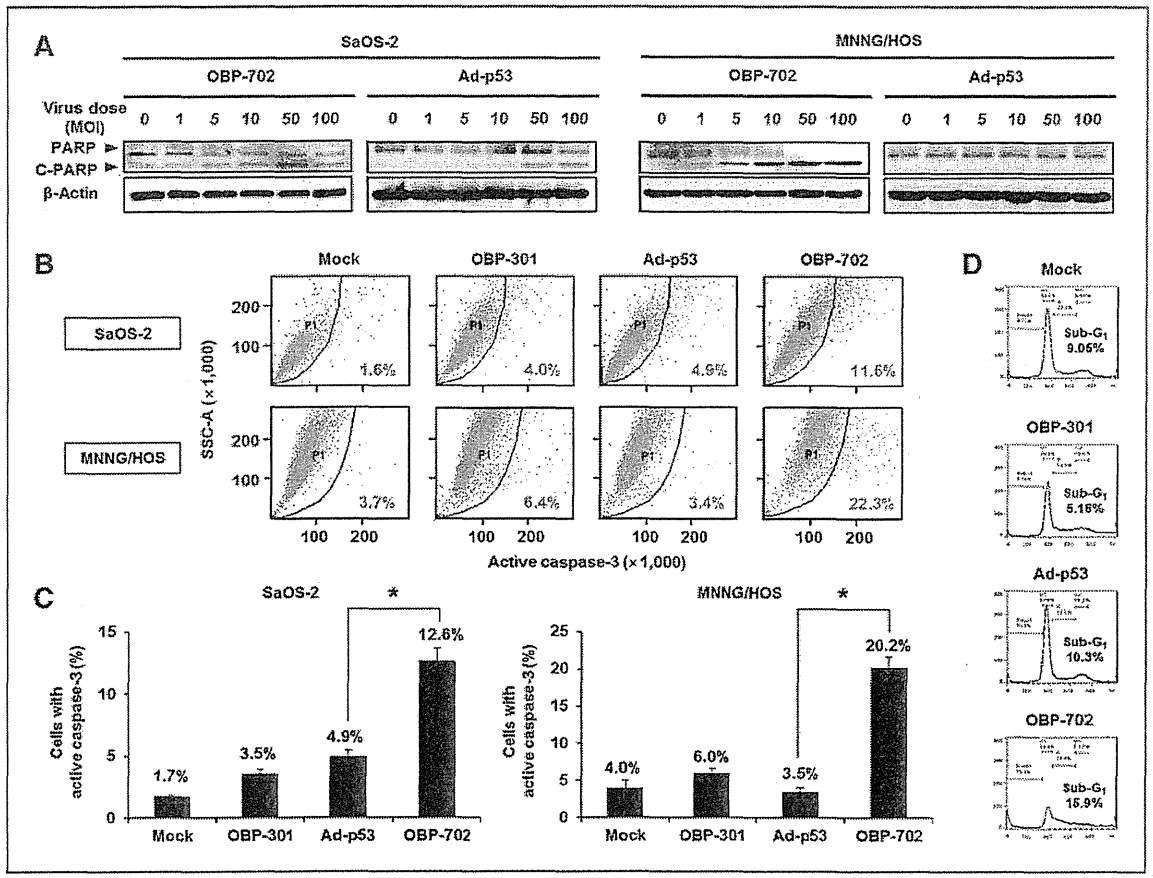

Figure 2. OBP-702 induces increased apoptosis when compared with OBP-301 or Ad-p53. A, OBP-301–resistant SaOS-2 and MNNG/HOS cells were infected with OBP-702 or Ad-p53 at the indicated MOIs for 72 hours. Cell lysates were subjected to Western blot analysis for the C-PARP and PARP. β-Actin was assayed as a loading control. B–D, SaOS-2 and MNNG/HOS cells were infected with OBP-702, OBP-301, or Ad-p53 at an MOI of 10 for 48 hours. Mock-infected cells were used as control. Caspase-3 activation was quantified using the flow cytometric analysis. Representative flow cytometric data are shown in B. The mean percentage of SaOS-2 cells and MNNG/HOS cells that express active caspase-3 was calculated on the basis of 3 independent experiments (C). The cell-cycle state was analyzed by flow cytometry in SaOS-2 cells after staining with propidium iodide. Representative cell-cycle data are shown (D). The percentage of sub-G_1 population was expressed in each graph. Bars, SD. Statistical significance was determined using Student *t* test. *, $P < 0.05$.

cells (31). Therefore, we next investigated whether OBP-702 induces more profound autophagy than does OBP-301. Western blot analysis revealed that OBP-702 infection showed increased autophagy, which was confirmed by conversion of LC3-I to LC3-II (increased ratio of LC3-II/LC3-I) and p62 downregulation, when compared with OBP-301 in MNNG/HOS cells (Fig. 4A). Moreover, the expression level of the p53-induced modulator of autophagy, DRAM (32), was decreased after OBP-301 infection, but its expression was maintained after OBP-702 infection (Fig. 4A). As p53-mediated p21 overexpression is known to inhibit both apoptosis and autophagy (17, 18), we further evaluated whether miR-mediated p21 suppression is involved in the enhancement of p53-mediated autophagy induction. Ad-p53–induced autophagy was enhanced by *miR-93*- and *miR-106b*–mediated p21 suppression (Fig. 4B). These results suggest that OBP-702 induces more profound autophagy than does OBP-301 and that this effect occurs via p53-mediated DRAM activation and miR-mediated p21 suppression.

Enhanced antitumor effect of OBP-702 in an orthotopic xenograft tumor model

Finally, to assess the *in vivo* antitumor effect of OBP-702, we used an orthotopic MNNG/HOS tumor xenograft model. OBP-702, OBP-301, Ad-p53, or PBS were intratumorally injected for 3 cycles every 2 days. OBP-702 administration significantly suppressed tumor growth when compared with OBP-301, Ad-p53, or PBS in an orthotopic MNNG/HOS tumor model (Fig. 5A and B). 3D-CT examination revealed that OBP-702–treated tumors had less bone destruction than did OBP-301- or Ad-p53–treated

Published OnlineFirst January 11, 2013; DOI: 10.1158/1535-7163.MCT-12-0869

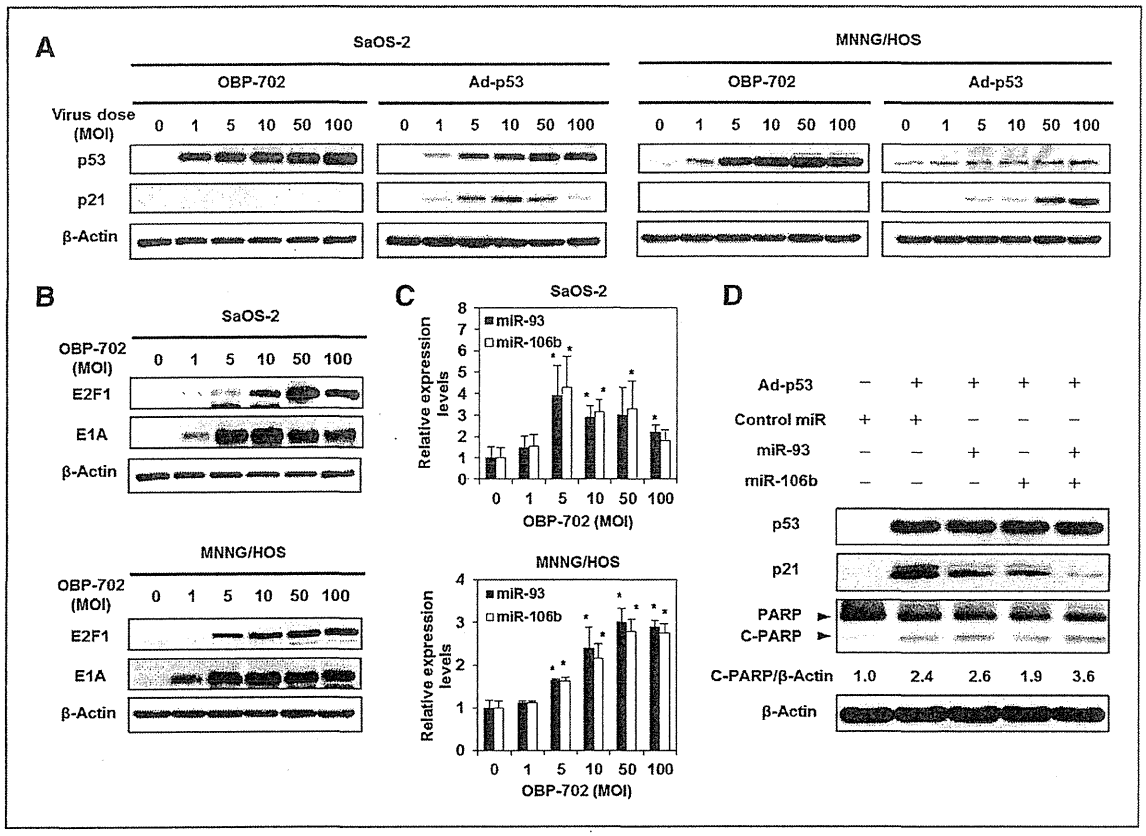

Figure 3. OBP-702 induces p53 overexpression with E1A-mediated p21 suppression via *miR-93* and *miR-106b* activation. A, expression of the p53 and p21 proteins in SaOS-2 and MNNG/HOS cells infected with OBP-702 or Ad-p53 at the indicated MOIs for 72 hours was assessed using Western blot analysis. B, expression of the E2F1 and viral E1A proteins in SaOS-2 and MNNG/HOS cells infected with OBP-702 at the indicated MOIs for 72 hours was assessed using Western blot analysis. C, expression of *miR-93* and *miR-106b* was assayed using qRT-PCR in SaOS-2 cells infected with OBP-702 at the indicated MOIs for 72 hours on 3 independent experiments. The values of *miR-93* and *miR-106b* at 0 MOI were set at 1, and the relative levels of *miR-93* and *miR-106b* at the indicated MOIs were plotted as fold induction. Bars, SD. Statistical significance was determined by Student *t* test. *, $P < 0.05$. D, SaOS-2 cells were transfected with 10 nmol/L *miR-93*, *miR-106*, or control miRNA 24 hours before Ad-p53 infection at an MOI of 100. At 48 hours after Ad-p53 infection, the expression levels of p53, p21, PARP, and C-PARP were examined by Western blot analysis. β-Actin was assayed as a loading control. By using ImageJ software, the expression level of C-PARP protein was calculated relative to its expression in the control miR–treated cells, whose expression level was designated as 1.0.

tumors (Fig. 5C). On histopathologic analysis, there were large necrotic areas in OBP-702–treated tumors but not in OBP-301- or Ad-p53–treated tumors (Fig. 5D). Moreover, the expression of the cell proliferation marker, Ki67, was also decreased, especially in OBP-702–treated tumor cells (Supplementary Fig. S6). These results suggest that OBP-702 eliminates tumor tissues more efficiently when compared with OBP-301 or Ad-p53.

Discussion

We previously reported that telomerase-specific replication-competent oncolytic adenovirus OBP-301 has strong antitumor activity in a variety of human epithelial and nonepithelial malignant cells (12, 14, 27). However, some human osteosarcoma cells were resistant to the cytopathic activity of OBP-301 (14). In this study, we showed that a novel p53-expressing oncolytic adenovirus, OBP-702, had increased *in vitro* and *in vivo* antitumor effects than did OBP-301 in human osteosarcoma cells (Fig. 1 and 5). OBP-702 induced increased apoptosis in association with p53 upregulation and p21 downregulation when compared with replication-deficient Ad-p53 (Fig. 2 and 3A). E1A-dependent upregulation of *miR-93* and *miR-106b* was involved in OBP-702–mediated suppression of p21 expression (Fig. 3). Moreover, p53-mediated DRAM activation with p21 suppression enhanced oncolytic adenovirus-mediated autophagy induction (Fig. 4). Recent studies suggest that transgene-expressing armed oncolytic adenoviruses are a promising antitumor strategy for induction of oncolytic and transgene-induced cell death (33). Although p53 overexpression has been shown to enhance antitumor

Published OnlineFirst January 11, 2013; DOI: 10.1158/1535-7163.MCT-12-0869

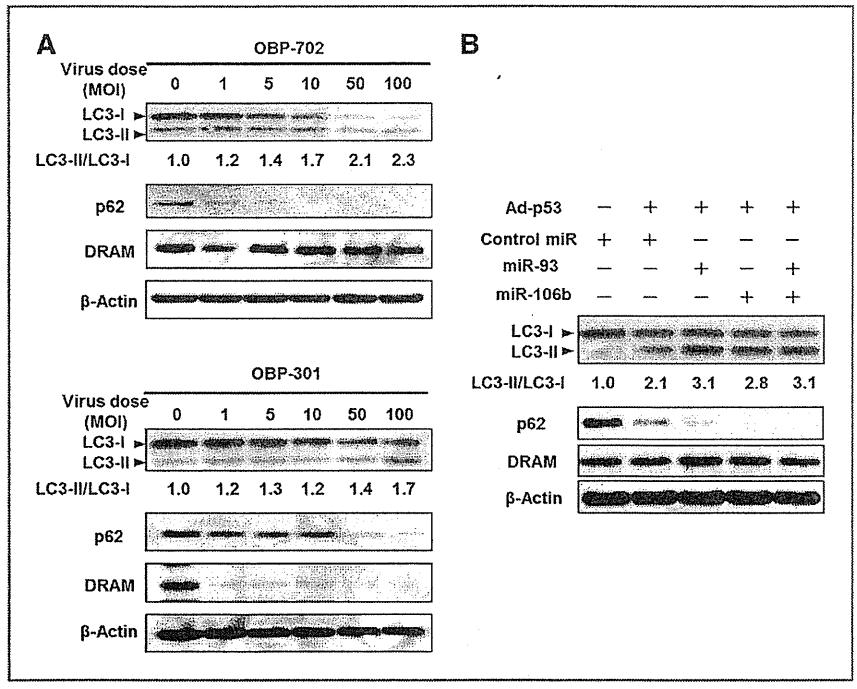

Figure 4. OBP-702 induces increased autophagy when compared with OBP-301. A, MNNG/HOS cells were infected with OBP-702 or OBP-301 at the indicated MOIs for 72 hours. Cell lysates were subjected to Western blot analysis for LC3, p62, and DRAM. B, SaOS-2 cells were transfected with 10 nmol/L *miR-93*, *miR-106*, or control miRNA 24 hours before Ad-p53 infection. At 48 hours after Ad-p53 infection at an MOI of 100, the expression levels of LC3, p62, and DRAM were examined by Western blot analysis. β-Actin was assayed as a loading control. By using ImageJ software, the ratio of LC3-II/LC3-I expressions was calculated relative to its expression in the mock-infected cells, whose expression level was designated as 1.0.

activity of oncolytic adenoviruses (34), the molecular mechanisms by which p53 mediates enhancement of the antitumor effect remain unclear. Recently, we reported that OBP-702 induces profound apoptosis through p53-dependent BAX upregulation and E1A-dependent p21 and MDM2 downregulation in epithelial malignant cells (26). Thus, oncolytic adenovirus-mediated p53 overexpression likely induces dual apoptotic and autophagic cell death pathways through p53-dependent BAX/DRAM activation and E1A-dependent p21/MDM2 suppression with E2F1-inducible *miR-93/106b* upregulation (Fig. 6).

OBP-702 efficiently suppressed the cell viability of both OBP-301–sensitive and -resistant osteosarcoma cells (Fig. 1). We previously reported that OBP-301–resistant SaOS-2 cells have no *hTERT* mRNA expression (Table 1), suggesting that SaOS-2 cells maintain telomere length through alternative lengthening of telomeres (ALT). As *hTERT* gene promoter is used for tumor-specific replication of OBP-301, ALT-type human osteosarcoma cells such as SaOS-2 cells may be resistant to OBP-301. However, ALT-type SaOS-2 cells showed similar sensitivity to OBP-702 as well as non–ALT-type MNNG/HOS cells (Fig. 1 and Table 1). These results suggest that p53 overexpression overcomes resistance to OBP-301 in ALT-type SaOS-2 cells. As the replication rate of OBP-702 was almost similar that of OBP-301 in ALT-type SaOS-2 cells (Supplementary Fig. S2), p53-induced cell death pathway would suppress the cell viability of ALT-type human osteosarcoma cells.

OBP-702–mediated p53 overexpression induced 2 types of programmed cell deaths (i.e., apoptosis and autophagy), thereby contributing to the enhancement of the antitumor effect of OBP-301 in human osteosarcoma cells (Fig. 2 and 4). As p53 downstream target p21 functions as a suppressor of apoptosis and autophagy (17, 18), p21 suppression may be a critical factor to induce dual programmed cell death pathways in response p53 overexpression. Suppression of p21 expression by genetic deletion or artificial p21 target microRNA has been shown to enhance the Ad-p53–induced apoptosis (18, 35). Inactivation of p21 by adenoviral E1A has been shown to enhance apoptosis in chemotherapeutic drug-treated human colon cancer cells that overexpress p53 (36). Genetic deletion of p21 has been also shown to induce autophagy in mouse embryonic fibroblasts treated with C (2)-ceramide or γ-irradiation (17). In contrast, p21 overexpression inhibited the Ad-p53–mediated apoptosis induction (18). Thus, E1A-mediated p21 downregulation would enhance p53-induced apoptosis and autophagy in OBP-702–infected cells.

E1A-dependent E2F1 activation and subsequent upregulation of E2F1-inducible miRNAs efficiently suppressed p21 expression, leading to the enhancement of p53-induced apoptosis and autophagy, in OBP-702–infected osteosarcoma cells (Figs. 2–4). Recent studies suggest that the cross-talk between p53 and E2F1 play a role in the regulation of diverse cell fates (37). For example, co-expression of p53 and E2F1 contributes to induction of apoptosis (38, 39). We previously showed

Published OnlineFirst January 11, 2013; DOI: 10.1158/1535-7163.MCT-12-0869

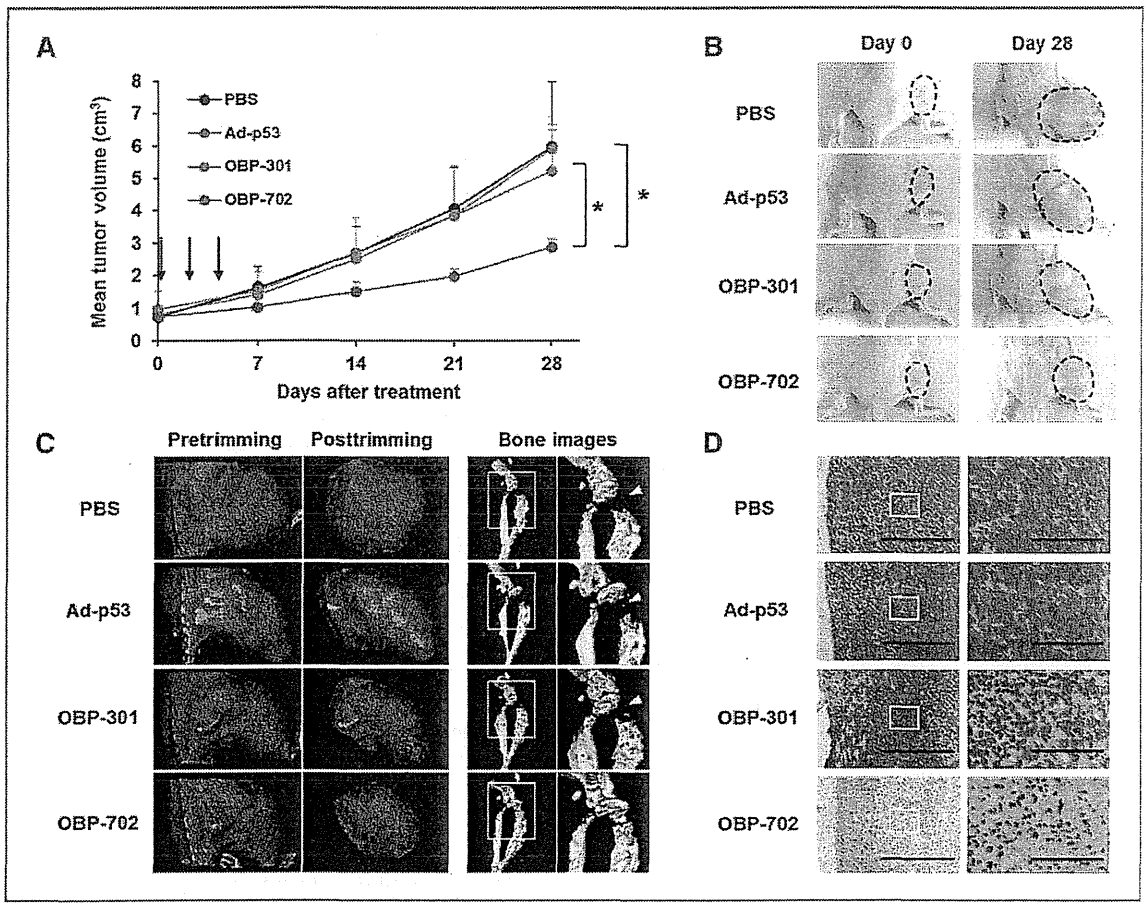

Figure 5. Antitumor effect of OBP-702 in an orthotopic MNNG/HOS osteosarcoma xenograft model. A, athymic nude mice were inoculated intratibially with MNNG/HOS cells (5×10^6 cells/site). Twenty-one days after inoculation (designated as day 0), Ad-p53, OBP-301, or OBP-702 were injected into the tumor with 1×10^8 PFUs on days 0, 2, and 4 (black arrows). PBS was used as a control. Three mice were used for each group. Each tumor volume was assessed by CT examination. Tumor growth was expressed as mean tumor volume ± SD. Statistical significance was determined by Student *t* test. *, $P < 0.05$. B, macroscopic appearance of MNNG/HOS tumors in nude mice on days 0 and 28 after treatment with PBS, Ad-p53, OBP-301, or OBP-702. Tumor masses are outlined by a dotted line. C, 3D-CT images of MNNG/HOS tumors. The tumor volumes were calculated by the image viewer (INTAGE Realia) based on 3D-CT images of tumors after trimming. The white arrowheads indicate the osteolytic areas within tumor tissues treated with PBS, Ad-p53, or OBP-301. Left side images are low magnification and right side images are high magnification of the area outlined by a white square. D, histologic analysis of the MNNG/HOS tumors. Tumor tissues were obtained on day 28 after first treatment with PBS, Ad-p53, OBP-301, or OBP-702. Paraffin-embedded sections of MNNG/HOS tumors were stained with hematoxylin and eosin solutions. There were large necrotic areas in MNNG/HOS tumors treated with OBP-702. Left side images are low magnification and right side images are high magnification of the area outlined by a white square. Left scale bars, 500 μm. Right scale bars, 100 μm.

that E2F1 enhanced Ad-p53–mediated apoptosis through p14ARF-dependent MDM2 downregulation (39) and that OBP-702 infection showed E1A-dependent MDM2 downregulation in association with apoptosis (26). Recently, E2F1 has been shown to suppress MDM2 expression by suppressing the promoter activity (40) or by inducing upregulation of *miR-25/32*, which targets MDM2 (41). Furthermore, E2F1-inducible *miR-93/106b* enhanced Ad-p53–induced apoptosis and autophagy via p21 suppression (Figs. 3D and 4B). Therefore, the cooperation between the MDM2/p53/p21 pathway and the E2F1/miRNA pathway may be involved in the induction of apoptotic and autophagic cell death in response to OBP-702.

OBP-702–mediated p53 overexpression enhanced autophagy that was induced by oncolytic adenovirus in human osteosarcoma cells. OBP-702 infection induced increased expression of DRAM and decreased expression of p62 when compared with OBP-301 (Fig. 4), suggesting that OBP-702–mediated p53 overexpression enhances autophagy through DRAM activation. We recently reported that OBP-301 induces autophagy through E1A-dependent activation of E2F1/*miR-7* pathway and subsequent suppression of EGF receptor

Published OnlineFirst January 11, 2013; DOI: 10.1158/1535-7163.MCT-12-0869

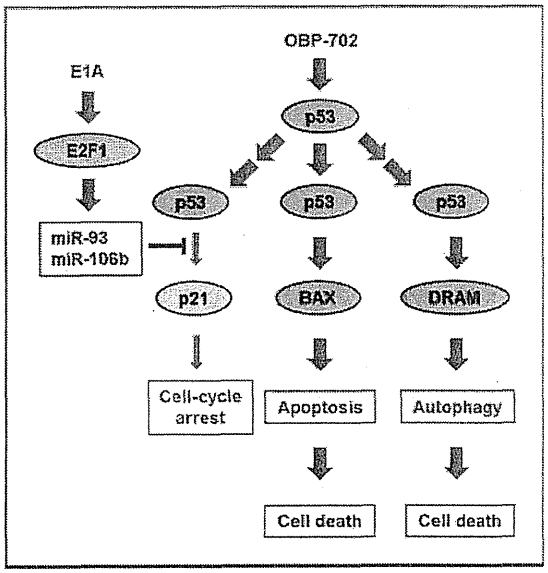

Figure 6. Outline of OBP-702–mediated induction of dual programmed cell death pathways. OBP-702 infection induces apoptosis and autophagy, leading to cell death, through p53-dependent BAX/DRAM upregulation and E1A-dependent p21 downregulation via E2F1-inducible *miR-93/106b* activation.

(EGFR; ref. 31). Restoration of p53 expression enhances the sensitivity to EGFR inhibitors in human cancer cells (42). Moreover, EGFR downregulation by transfection of specific antisense oligonucleotide promotes the differentiation status of human osteosarcoma U2OS cells (43). Thus, OBP-702 may induce differentiation as well as cell death through autophagy activation by DRAM upregulation and EGFR downregulation in human osteosarcoma cells.

The 3D-CT imaging system was a useful method to assess both tumor volume and bone destruction status in MNNG/HOS tumors. OBP-702–treated tumors were smaller and had less bone destruction than PBS-, Ad-p53-, or OBP-301–treated tumors (Fig. 5A and C). Recent reports have suggested that zoledronic acid suppresses tumor growth as well as osteolytic components in human osteosarcoma xenograft tumor models (44, 45). These results suggest that combination therapy with OBP-702 and zoledronic acid may be more effective and more protective against bone destruction in human osteosarcomas. Further study using a 3D-CT imaging system may provide important information about bone destruction status in osteosarcomas treated with OBP-702 and zoledronic acid.

Adenovirus-mediated *p53* gene therapy exerts an antitumor effect in human osteosarcoma cells (46). However, the antitumor activity of replication-deficient Ad-p53 is limited in some human osteosarcoma cells (47). Ad-p53–mediated p53 overexpression increases the sensitivity of human osteosarcoma cells to the chemotherapeutic drugs, cisplatin and doxorubicin (48). A synergistic antitumor effect between doxorubicin and roscovitine was also associated with autophagy induction in human osteosarcoma U2OS cells (49). As OBP-702 induced more profound apoptosis and autophagy than did OBP-301 or Ad-p53 (Fig. 2 and 4), combination therapy with OBP-702 and chemotherapeutic agents may be more effective than monotherapy with OBP-702. Moreover, a recent report has shown that p53-armed replication-competent oncolytic adenovirus is a safe antitumor agent in rodents and non-human primates (50). However, for clinical application of OBP-702, it must be necessary to establish the systemic delivery method and confirm the host biologic contributions in patients with cancer. Although there are some unsolved issues, the combination of p53-armed oncolytic adenovirus and chemotherapy may provide us a promising antitumor strategy against human osteosarcoma cells.

In conclusion, we clearly showed that the p53-expressing oncolytic adenovirus OBP-702 has a much stronger antitumor effect than does OBP-301. Oncolytic adenovirus-mediated *p53* gene transduction may induce dual apoptotic and autophagic cell death pathways through p53-dependent activation of cell death inducers and E1A-dependent suppression of cell death inhibitors, resulting in the enhancement of antitumor effect.

Disclosure of Potential Conflicts of Interest

Y. Urata is President & CEO of Oncolys BioPharma, Inc., the manufacturer of OBP-301 (Telomelysin). H. Tazawa and T. Fujiwara are consultants of Oncolys BioPharma, Inc. No potential conflicts of interest were disclosed by the other authors.

Authors' Contributions

Conception and design: J. Hasei, F. Uno, S. Kagawa, T. Ozaki, T. Fujiwara
Development of methodology: J. Hasei, F. Uno, S. Kagawa
Acquisition of data (provided animals, acquired and managed patients, provided facilities, etc.): J. Hasei, H. Tazawa, S. Osaki, Y. Yamakawa, A. Yoshida, T. Onishi, T. Ozaki
Analysis and interpretation of data (e.g., statistical analysis, biostatistics, computational analysis): J. Hasei, H. Tazawa, T. Fujiwara
Writing, review, and/or revision of the manuscript: J. Hasei, H. Tazawa, T. Kunisada, Y. Urata, T. Fujiwara
Administrative, technical, or material support (i.e., reporting or organizing data, constructing databases): H. Tazawa, T. Kunisada, Y. Hashimoto, S. Kagawa, Y. Urata, T. Ozaki
Study supervision: T. Sasaki, T. Kunisada, F. Uno, Y. Urata, T. Fujiwara

Acknowledgments

The authors thank Dr. Satoru Kyo (Kanazawa University) for providing the HOS and SaOS-2 cells and Tomoko Sueishi for her excellent technical support.

Grant Support

This study was supported by grants-in-aid from the Ministry of Education, Science, and Culture, Japan (T. Fujiwara) and grants from the Ministry of Health and Welfare, Japan (T. Fujiwara), and in part by the National Cancer Center Research and Development Fund (23-A-10) (T. Ozaki).

The costs of publication of this article were defrayed in part by the payment of page charges. This article must therefore be hereby marked *advertisement* in accordance with 18 U.S.C. Section 1734 solely to indicate this fact.

Received August 30, 2012; revised December 27, 2012; accepted December 29, 2012; published OnlineFirst January 11, 2013.

Published OnlineFirst January 11, 2013; DOI: 10.1158/1535-7163.MCT-12-0869

References

1. Ottaviani G, Jaffe N. The etiology of osteosarcoma. Cancer Treat Res 2009;152:15–32.
2. Damron TA, Ward WG, Stewart A. Osteosarcoma, chondrosarcoma, and Ewing's sarcoma: National Cancer Data Base Report. Clin Orthop Relat Res 2007;459:40–7.
3. Lewis IJ, Nooij MA, Whelan J, Sydes MR, Grimer R, Hogendoorn PC, et al. Improvement in histologic response but not survival in osteosarcoma patients treated with intensified chemotherapy: a randomized phase III trial of the European Osteosarcoma Intergroup. J Natl Cancer Inst 2007;99:112–28.
4. Bacci G, Longhi A, Versari M, Mercuri M, Briccoli A, Picci P. Prognostic factors for osteosarcoma of the extremity treated with neoadjuvant chemotherapy: 15-year experience in 789 patients treated at a single institution. Cancer 2006;106:1154–61.
5. Bielack SS, Kempf-Bielack B, Delling G, Exner GU, Flege S, Helmke K, et al. Prognostic factors in high-grade osteosarcoma of the extremities or trunk: an analysis of 1,702 patients treated on neoadjuvant cooperative osteosarcoma study group protocols. J Clin Oncol 2002; 20:776–90.
6. Siegel R, Naishadham D, Jemal A. Cancer statistics, 2012. CA Cancer J Clin 2012;62:10–29.
7. Buseman CM, Wright WE, Shay JW. Is telomerase a viable target in cancer? Mutat Res 2012;730:90–7.
8. Artandi SE, DePinho RA. Telomeres and telomerase in cancer. Carcinogenesis 2010;31:9–18.
9. Umehara N, Ozaki T, Sugihara S, Kunisada T, Morimoto Y, Kawai A, et al. Influence of telomerase activity on bone and soft tissue tumors. J Cancer Res Clin Oncol 2004;130:411–6.
10. Aogi K, Woodman A, Urquidi V, Mangham DC, Tarin D, Goodison S. Telomerase activity in soft-tissue and bone sarcomas. Clin Cancer Res 2000;6:4776–81.
11. Nakayama J, Tahara H, Tahara E, Saito M, Ito K, Nakamura H, et al. Telomerase activation by hTRT in human normal fibroblasts and hepatocellular carcinomas. Nat Genet 1998;18:65–8.
12. Kawashima T, Kagawa S, Kobayashi N, Shirakiya Y, Umeoka T, Teraishi F, et al. Telomerase-specific replication-selective virotherapy for human cancer. Clin Cancer Res 2004;10:285–92.
13. Nemunaitis J, Tong AW, Nemunaitis M, Senzer N, Phadke AP, Bedell C, et al. A phase I study of telomerase-specific replication competent oncolytic adenovirus (telomelysin) for various solid tumors. Mol Ther 2010;18:429–34.
14. Sasaki T, Tazawa H, Hasei J, Kunisada T, Yoshida A, Hashimoto Y, et al. Preclinical evaluation of telomerase-specific oncolytic virotherapy for human bone and soft tissue sarcomas. Clin Cancer Res 2011;17:1828–38.
15. Li G, Kawashima H, Ogose A, Ariizumi T, Xu Y, Hotta T, et al. Efficient virotherapy for osteosarcoma by telomerase-specific oncolytic adenovirus. J Cancer Res Clin Oncol 2011;137:1037–51.
16. Vousden KH, Prives C. Blinded by the light: the growing complexity of p53. Cell 2009;137:413–31.
17. Fujiwara K, Daido S, Yamamoto A, Kobayashi R, Yokoyama T, Aoki H, et al. Pivotal role of the cyclin-dependent kinase inhibitor p21WAF1/CIP1 in apoptosis and autophagy. J Biol Chem 2008;283:388–97.
18. Gorospe M, Cirielli C, Wang X, Seth P, Capogrossi MC, Holbrook NJ. p21(Waf1/Cip1) protects against p53-mediated apoptosis of human melanoma cells. Oncogene 1997;14:929–35.
19. Blagosklonny MV, el-Deiry WS. In vitro evaluation of a p53-expressing adenovirus as an anti-cancer drug. Int J Cancer 1996;67:386–92.
20. Zeng Y, Prabhu N, Meng R, Eldeiry W. Adenovirus-mediated p53 gene therapy in nasopharyngeal cancer. Int J Oncol 1997;11:221–6.
21. Clayman GL, el-Naggar AK, Lippman SM, Henderson YC, Frederick M, Merritt JA, et al. Adenovirus-mediated p53 gene transfer in patients with advanced recurrent head and neck squamous cell carcinoma. J Clin Oncol 1998;16:2221–32.
22. Swisher SG, Roth JA, Nemunaitis J, Lawrence DD, Kemp BL, Carrasco CH, et al. Adenovirus-mediated p53 gene transfer in advanced non-small-cell lung cancer. J Natl Cancer Inst 1999;91:763–71.
23. Shimada H, Matsubara H, Shiratori T, Shimizu T, Miyazaki S, Okazumi S, et al. Phase I/II adenoviral p53 gene therapy for chemoradiation resistant advanced esophageal squamous cell carcinoma. Cancer Sci 2006;97:554–61.
24. Fujiwara T, Tanaka N, Kanazawa S, Ohtani S, Saijo Y, Nukiwa T, et al. Multicenter phase I study of repeated intratumoral delivery of adenoviral p53 in patients with advanced non-small-cell lung cancer. J Clin Oncol 2006;24:1689–99.
25. Sakai R, Kagawa S, Yamasaki Y, Kojima T, Uno F, Hashimoto Y, et al. Preclinical evaluation of differentially targeting dual virotherapy for human solid cancer. Mol Cancer Ther 2010;9:1884–93.
26. Yamasaki Y, Tazawa H, Hashimoto Y, Kojima T, Kuroda S, Yano S, et al. A novel apoptotic mechanism of genetically engineered adenovirus-mediated tumour-specific p53 overexpression through E1A-dependent p21 and MDM2 suppression. Eur J Cancer 2012;48: 2282–91.
27. Hashimoto Y, Watanabe Y, Shirakiya Y, Uno F, Kagawa S, Kawamura H, et al. Establishment of biological and pharmacokinetic assays of telomerase-specific replication-selective adenovirus. Cancer Sci 2008;99:385–90.
28. Bagchi S, Raychaudhuri P, Nevins JR. Adenovirus E1A proteins can dissociate heteromeric complexes involving the E2F transcription factor: a novel mechanism for E1A trans-activation. Cell 1990;62: 659–69.
29. Emmrich S, Putzer BM. Checks and balances: E2F-microRNA crosstalk in cancer control. Cell Cycle 2010;9:2555–67.
30. Petrocca F, Vecchione A, Croce CM. Emerging role of miR-106b-25/miR-17-92 clusters in the control of transforming growth factor beta signaling. Cancer Res 2008;68:8191–4.
31. Tazawa H, Yano S, Yoshida R, Yamasaki Y, Sasaki T, Hashimoto Y, et al. Genetically engineered oncolytic adenovirus induces autophagic cell death through an E2F1-microRNA-7-epidermal growth factor receptor axis. Int J Cancer 2012;131:2939–50.
32. Crighton D, Wilkinson S, O'Prey J, Syed N, Smith P, Harrison PR, et al. DRAM, a p53-induced modulator of autophagy, is critical for apoptosis. Cell 2006;126:121–34.
33. Liu TC, Galanis E, Kirn D. Clinical trial results with oncolytic virotherapy: a century of promise, a decade of progress. Nat Clin Pract Oncol 2007;4:101–17.
34. van Beusechem VW, van den Doel PB, Grill J, Pinedo HM, Gerritsen WR. Conditionally replicative adenovirus expressing p53 exhibits enhanced oncolytic potency. Cancer Res 2002;62:6165–71.
35. Idogawa M, Sasaki Y, Suzuki H, Mita H, Imai K, Shinomura Y, et al. A single recombinant adenovirus expressing p53 and p21-targeting artificial microRNAs efficiently induces apoptosis in human cancer cells. Clin Cancer Res 2009;15:3725–32.
36. Chattopadhyay D, Ghosh MK, Mal A, Harter ML. Inactivation of p21 by E1A leads to the induction of apoptosis in DNA-damaged cells. J Virol 2001;75:9844–56.
37. Polager S, Ginsberg D. p53 and E2f: partners in life and death. Nat Rev Cancer 2009;9:738–48.
38. Wu X, Levine AJ. p53 and E2F-1 cooperate to mediate apoptosis. Proc Natl Acad Sci U S A 1994;91:3602–6.
39. Itoshima T, Fujiwara T, Waku T, Shao J, Kataoka M, Yarbrough WG, et al. Induction of apoptosis in human esophageal cancer cells by sequential transfer of the wild-type p53 and E2F-1 genes: involvement of p53 accumulation via ARF-mediated MDM2 down-regulation. Clin Cancer Res 2000;6:2851–9.
40. Tian X, Chen Y, Hu W, Wu M. E2F1 inhibits MDM2 expression in a p53-dependent manner. Cell Signal 2011;23:193–200.
41. Suh SS, Yoo JY, Nuovo GJ, Jeon YJ, Kim S, Lee TJ, et al. MicroRNAs/TP53 feedback circuitry in glioblastoma multiforme. Proc Natl Acad Sci U S A 2012;109:5316–21.
42. Huang S, Benavente S, Armstrong EA, Li C, Wheeler DL, Harari PM. p53 modulates acquired resistance to EGFR inhibitors and radiation. Cancer Res 2011;71:7071–9.
43. Salvatori L, Caporuscio F, Coroniti G, Starace G, Frati L, Russo MA, et al. Down-regulation of epidermal growth factor receptor induced by estrogens and phytoestrogens promotes the differentiation of U2OS human osteosarcoma cells. J Cell Physiol 2009;220: 35–44.

Published OnlineFirst January 11, 2013; DOI: 10.1158/1535-7163.MCT-12-0869

44. Dass CR, Choong PF. Zoledronic acid inhibits osteosarcoma growth in an orthotopic model. Mol Cancer Ther 2007;6:3263–70.
45. Labrinidis A, Hay S, Liapis V, Ponomarev V, Findlay DM, Evdokiou A. Zoledronic acid inhibits both the osteolytic and osteoblastic components of osteosarcoma lesions in a mouse model. Clin Cancer Res 2009;15:3451–61.
46. Ternovoi VV, Curiel DT, Smith BF, Siegal GP. Adenovirus-mediated p53 tumor suppressor gene therapy of osteosarcoma. Lab Invest 2006;86:748–66.
47. Hellwinkel OJ, Muller J, Pollmann A, Kabisch H. Osteosarcoma cell lines display variable individual reactions on wildtype p53 and Rb tumour-suppressor transgenes. J Gene Med 2005;7:407–19.
48. Ganjavi H, Gee M, Narendran A, Parkinson N, Krishnamoorthy M, Freedman MH, et al. Adenovirus-mediated p53 gene therapy in osteosarcoma cell lines: sensitization to cisplatin and doxorubicin. Cancer Gene Ther 2006;13:415–9.
49. Lambert LA, Qiao N, Hunt KK, Lambert DH, Mills GB, Meijer L, et al. Autophagy: a novel mechanism of synergistic cytotoxicity between doxorubicin and roscovitine in a sarcoma model. Cancer Res 2008;68:7966–74.
50. Su C, Cao H, Tan S, Huang Y, Jia X, Jiang L, et al. Toxicology profiles of a novel p53-armed replication-competent oncolytic adenovirus in rodents, felids, and nonhuman primates. Toxicol Sci 2008;106:242–50.

Molecular Cancer Therapeutics

Correction: Dual Programmed Cell Death Pathways Induced by p53 Transactivation Overcome Resistance to Oncolytic Adenovirus in Human Osteosarcoma Cells

In this article (Mol Cancer Ther 2013;12:314–25), which appeared in the March 2013 issue of *Molecular Cancer Therapeutics* (1), the authors regret that the actin panel for A-p53 in Fig. 3A is incorrect. We used the same membrane for analyzing multiple protein expression and, therefore, the actin panel should be the same for different proteins, but not for different cell lines. The corresponding author apologizes for the error made during the revision process. The correct actin panel for Ad-p53 is used in the last panel of Fig. 3A. Please see the correct Fig. 3A below.

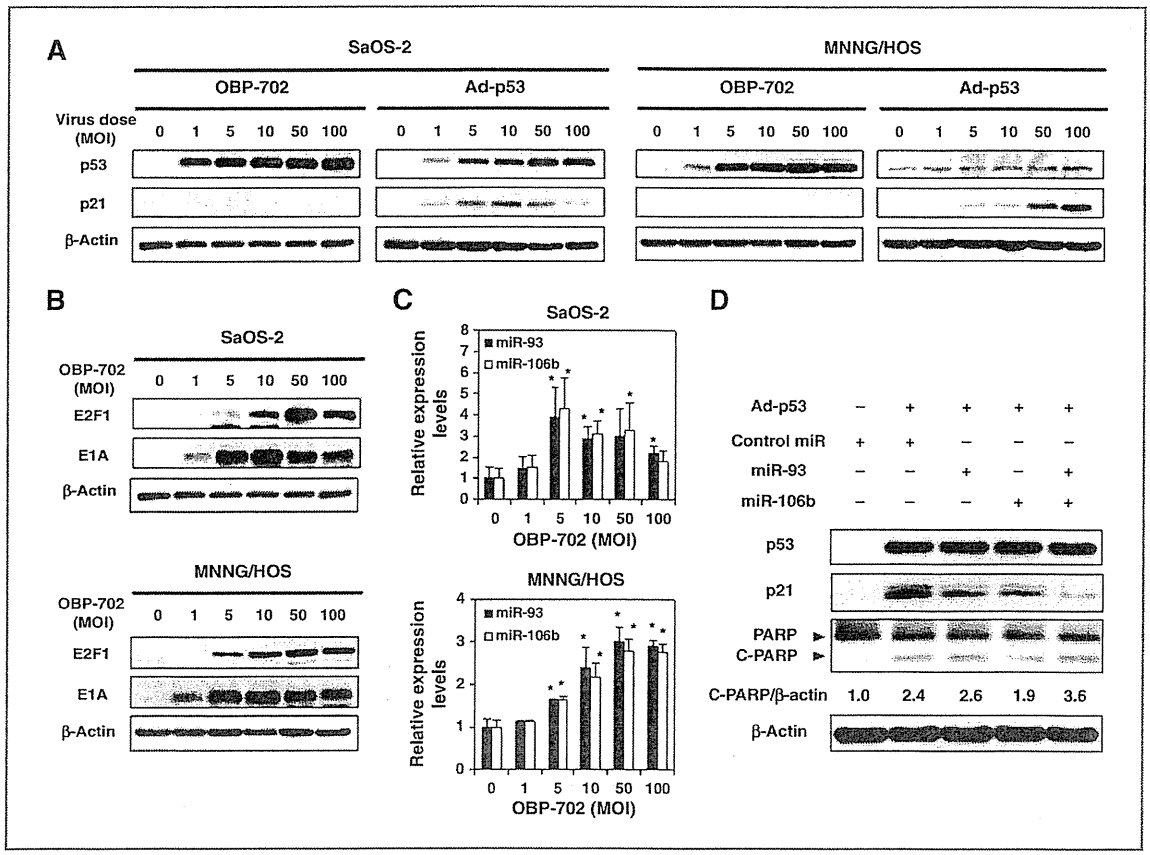

Figure 3. OBP-702 induces p53 overexpression with E1A-mediated p21 suppression via miR-93 and miR-106b activation. A, expression of the p53 and p21 proteins in SaOS-2 and MNNG/HOS cells infected with OBP-702 or Ad-p53 at the indicated MOIs for 72 hours was assessed using Western blot analysis. B, expression of the E2F1 and viral E1A proteins in SaOS-2 and MNNG/HOS cells infected with OBP-702 at the indicated MOIs for 72 hours was assessed using Western blot analysis. C, expression of miR-93 and miR-106b was assayed using qRT-PCR in SaOS-2 cells infected with OBP-702 at the indicated MOIs for 72 hours in 3 independent experiments. The values of miR-93 and miR-106b at 0 MOI were set at 1, and the relative levels of miR-93 and miR-106b at the indicated MOIs were plotted as fold induction. Bars, SD. Statistical significance was determined by Student *t* test; *, $P < 0.05$. D, SaOS-2 cells were transfected with 10 nmol/L miR-93, miR-106, or control miRNA 24 hours before Ad-p53 infection at an MOI of 100. Forty-eight hours after Ad-p53 infection, the expression levels of p53, p21, PARP, and C-PARP were examined by Western blot analysis. β-Actin was assayed as a loading control. By using ImageJ software, the expression level of C-PARP protein was calculated relative to its expression in the control miR–treated cells, whose expression level was designated as 1.0.

Reference

1. Hasei J, Sasaki T, Tazawa H, Osaki S, Yamakawa Y, Kunisada T, et al., Dual programmed cell death pathways induced by p53 transactivation overcome resistance to oncolytic adenovirus in human osteosarcoma cells. Mol Cancer Ther 2013;12:314–25.

Published OnlineFirst August 14, 2013.
doi: 10.1158/1535-7163.MCT-13-0600

Serum miR-210 as a potential biomarker of early clear cell renal cell carcinoma

HIDETO IWAMOTO[1], YUSUKE KANDA[2], TAKEHIRO SEJIMA[1], MITSUHIKO OSAKI[2], FUTOSHI OKADA[2] and ATSUSHI TAKENAKA[1]

Departments of [1]Surgery, Division of Urology and [2]Biomedical Sciences, Division of Pathological Biochemistry, Faculty of Medicine, Tottori University, Tottori 683-8503, Japan

Received June 7, 2013; Accepted July 19, 2013

DOI: 10.3892/ijo.2013.2169

Abstract. Early detection and treatment are critical in the management of renal cell carcinoma (RCC). However, there is no standard serum biomarker to facilitate early diagnosis or prognostic stratification in patients with RCC. Recent reports suggest that circulating microRNAs (miRNAs) have great potential as biomarkers for diagnosis and prognosis in patients with several types of cancers. Further, many studies using miRNA microarray analysis demonstrated that miR-210 expression in clear cell carcinoma (CCC), which is the largest subtype of RCC, was significantly upregulated in tumor tissue. Therefore, we investigated whether serum miR-210 could be a useful biomarker for the diagnosis and progression of CCC. This study included 34 CCC patients and 23 healthy controls (HC). First, we analyzed tissue miR-210 levels in tumor tissues and matched normal tissues from the 34 CCC patients. Second, we investigated the serum miR-210 levels in the 34 CCC patients and the 23 HC patients. Real-time polymerase chain reaction (PCR) was used to measure miRNA levels. Moreover, we examined the correlation between serum miR-210 levels and the clinicopathological parameters. Among patients with CCC, expression of miR-210 was higher in tumor tissues compared to normal tissues (P<0.001). Serum miR-210 levels were higher in CCC patients compared to HCs (P=0.001). Receiver operating characteristic (ROC) curve analysis showed an area under the ROC curve (AUC) of 0.77 (95% confidence interval, 0.65-0.89) and a sensitivity and specificity of 65 and 83%, respectively. In addition, there was no significant association between serum miR-210 levels and age, sex, tumor size or existence of metastasis at diagnosis among the 34 CCC patients. In conclusion, serum miR-210 upregulation may occur in the early stage of CCC and serum miR-210 can be a useful biomarker for early CCC in humans.

Correspondence to: Dr Mitsuhiko Osaki, Department of Biomedical Sciences, Division of Pathological Biochemistry, Faculty of Medicine, Tottori University, 86 Nishi-cho, Yonago, Tottori 683-8503, Japan
E-mail: osamitsu@med.tottori-u.ac.jp

Key words: microRNA, miR-210, renal cell carcinoma, clear cell carcinoma, serum biomarker, early diagnosis

Introduction

Renal cell carcinoma (RCC) is a common urological neoplasm of the adult kidney. The diagnostic modalities and therapeutic techniques for RCC continue to improve and the overall incidence and mortality of RCC has increased in the last 20 years (1). The 5-year survival rate is ~98% for stage I disease and ~50% for stage III disease (2), which underscore the importance of early detection and treatment of RCC. However, early detection of often difficult, because early-stage renal tumors are often asymptomatic and non-palpable. Therefore, the identification of non-invasive biomarkers for early-stage RCC would be of benefit. However, no accurate biomarker for RCC currently exists (3).

Recent studies suggest that microRNAs (miRNAs), which are non-protein-coding small RNAs, are involved in cancer progression and metastasis. MicroRNAs are ~22 nucleotides in length and regulate gene expression at the post-transcriptional level by binding to the untranslated region (3'UTR) of target mRNAs, leading to translational inhibition and/or mRNA degradation (4). Specific expression profiles of miRNAs in tissue have been reported in a variety of cancers, including RCC (5). Early studies suggested that miRNAs were strictly intracellular molecules, but more recent studies suggest that miRNAs are highly stable and abundant in the serum, urine and other body fluids. This is because exosomes likely protect miRNAs against degradation by RNase (6,7). Interestingly, serum miRNA levels are similar in men and women and do not vary with patient age (8).

Thus, circulating miRNAs might be good non-invasive biomarkers for diagnostic and prognostic considerations in a variety of cancers. Indeed, several studies have reported that specific circulating miRNAs were useful for distinguishing patients with cancer (e.g., colorectal cancer, breast cancer, prostate cancer) from healthy controls (HCs) (6,9,10). However, the number of studies regarding circulating miRNAs in patients with RCC is small.

Several studies using miRNA microarray analysis demonstrated that miR-210 expression in clear cell carcinoma (CCC), which is the largest subtype of RCC, was significantly

upregulated in tumor tissues and cell lines (11). In addition, some groups reported that miR-210 upregulation played an important role in tumorigenesis in various types of human cancers (12,13).

The goal of this study was to determine whether circulating miR-210 was a useful diagnostic biomarker for distinguishing CCC patients from HCs.

Materials and methods

Patients and sample collection. The study was approved by the ethics committee of Tottori University Hospital, Japan and all the patients provided written informed consent. We prospectively collected tissue and serum samples from patients undergoing radical nephrectomy or nephron-sparing surgery for renal tumors. Sample collection was performed between 2011 and 2013 at the Department of Urology, Tottori University Hospital. Thirty-four patients with histologically confirmed CCC and 23 HCs with no previous history of any cancer were included in this analysis. Detailed clinicopathological parameters of patients are summarized in Table I.

Tissue samples were obtained from tumor tissues and matched normal tissues from the same kidney specimen in patients with CCC. Immediately after resection, tissue samples were frozen in liquid nitrogen and stored at -80°C.

Blood samples were obtained prior to surgery. Serum was separated after centrifugation (3,000 rpm, 10 min) and stored at -80°C.

Total RNA isolation. Total RNA was extracted from tissue using the mirVana™ miRNA isolation kit (Ambion, USA) and from 200 μl of serum using the microRNA extractor SP kit (Wako, Japan) according to the manufacturer's recommendation (final elution volume, 50 μl). RNA quantity and purity were determined using a NanoDrop Spectrophotometer ND-1000 (Thermo Scientific, USA). The RNA samples were stored at -80°C until reverse transcription (RT) reaction.

Quantitative real-time PCR. Complementary DNA (cDNA) was synthetized from total RNA using the TaqMan MicroRNA RT kit (Applied Biosystems) and using miRNA-specific RT primers from the TaqMan MicroRNA assay (Applied Biosystems). RT reaction mixtures were incubated for 30 min at 16°C, 30 min at 42°C, 5 min at 85°C and then held at 4°C. Quantitative real-time PCR was performed using the TaqMan MicroRNA assay on the ABI PRISM 7900HT system (Applied Biosystems). All experiments were performed as specified in the manufacturer's protocols.

Statistical methods. Analysis of the real-time PCR data was done using SDS software, version 2.4 (Applied Biosystems). MicroRNA levels in tissue were normalized against miR-145 and microRNA levels in serum were normalized against miR-16. We confirmed that the expression of miR-145 in tissue and miR-16 in serum were not significantly different when comparing patients and HCs. The relative expression levels of miR-210 were determined by the equation: $2^{-\Delta CT}$ ($\Delta CT=C_{T\ miR\text{-}210}$ - $C^{T\ miR\text{-}145\ or\ 16}$). Statistical analyses were performed using PASW statistics 18 (SPSS, Chicago, IL, USA). Sensitivity, specificity and area under curve (AUC) for serum microRNA levels were determined using receiver operator characteristic (ROC) analysis. The relationship between clinicopathologic parameters and microRNA levels was examined using the Mann-Whitney U or Kruskal-Wallis test, as appropriate. P-values of <0.05 were considered to represent statistical significance.

Table I. Clinicopathological parameters.

	Serum samples	
	CCC (n=34)	HC (n=23)
Sex		
Male	26	11
Female	8	12
Age (years)		
Mean	66.5	53.5
Range	29-86	36-84
Pathological stage		
pT1a	17	-
pT1b	8	-
pT2a	3	-
pT2b	1	-
pT3a	4	-
pT3b	1	-
pT4	0	-
Lymph nodes metastasis	2	-
Distant metastasis	5	-
Grade		
G1	9	-
G2	24	-
G3	1	-

Results

Validation in tissue samples. Using real-time PCR, we first assessed tissue miR-210 levels normalized against miR-145 in 34 pairs of tumor tissues and matched normal tissues obtained from patients with CCC. Tissue miR-210 levels were significantly higher in tumor tissues than in normal tissues (P<0.001; Fig. 1A). There was no difference in the CT values for miR-145 when comparing tumor tissues and normal tissues (P=0.236; Fig. 1B). In 31 cases (92%), the miR-210 level in tumor tissues was increased by >2-fold when compared with that in normal tissues.

Validation in serum samples. We assessed serum miR-210 levels normalized against miR-16 in 34 CCC patients and 23 HCs. The 34 serum samples from CCC patients perfectly matched up with tissue samples described above. Serum miR-210 levels were significantly higher in CCC patients than in HCs (P=0.001; Fig. 2A). There was no significant difference

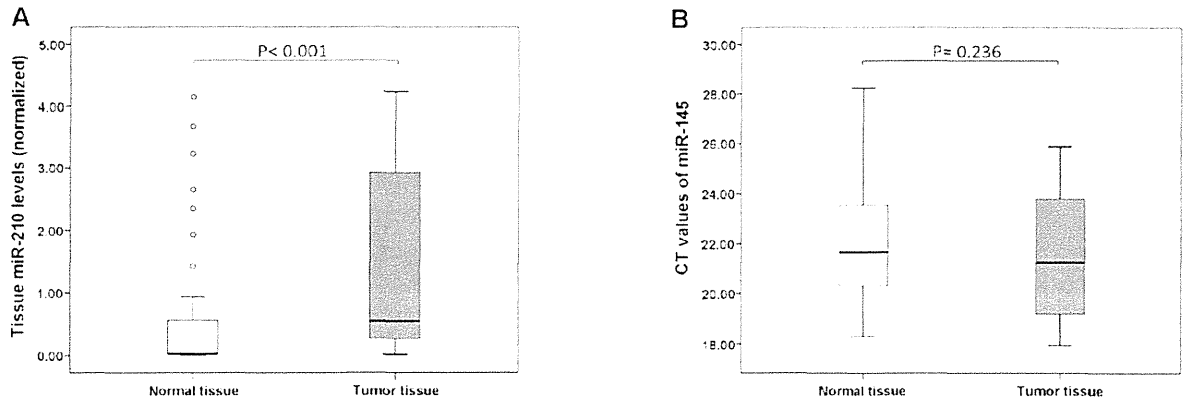

Figure 1. (A) Tissue miR-210 levels normalized against miR-145 in 34 pairs of tumor tissues and matched normal tissues taken from patients with clear cell carcinoma (CCC). The tissue miR-210 levels were significantly higher in tumor tissues than in normal tissues (P<0.001). (B) There was no significant differences in CT values of miR-145 when comparing tumor tissues and matched normal tissues.

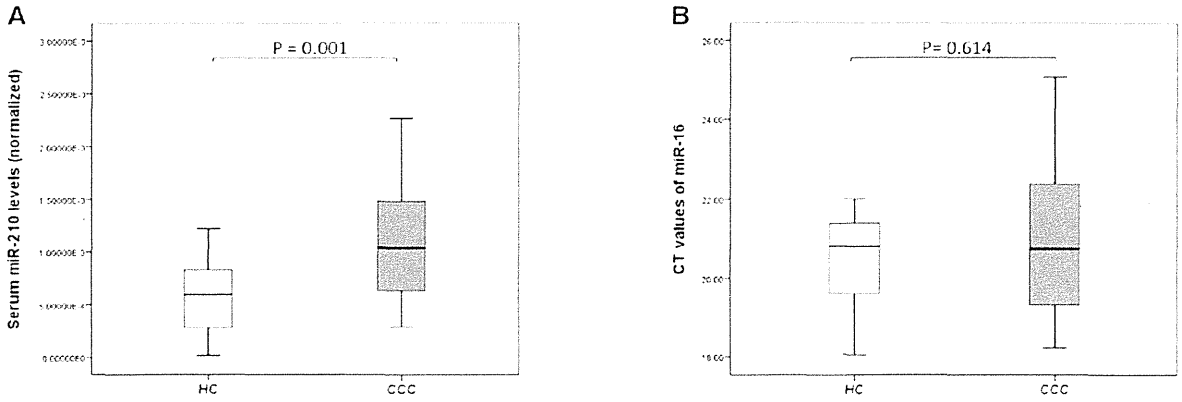

Figure 2. (A) Serum miR-210 levels normalized against miR-16 in 34 CCC patients and in 23 healthy controls (HCs). Serum miR-210 levels were significantly higher in CCC patients than in HCs (P=0.001). (B) There was no significant difference in CT values of miR-16 when comparing CCC patients and HCs.

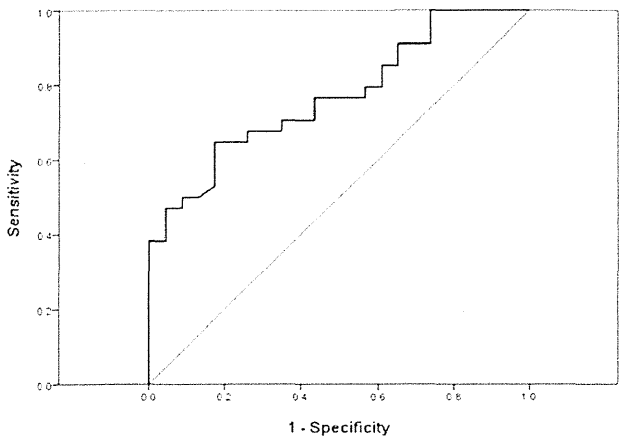

Figure 3. Receiver operating characteristic (ROC) analysis of serum miR-210 showed an area under the ROC curve (AUC) of 0.77 (95% confidence interval, 0.65-0.89) with a sensitivity and specificity of 65 and 83%, respectively.

in the CT values of miR-16 when comparing CCC patients and HCs (P=0.614; Fig. 2B).

ROC curve analysis indicated that the serum miR-210 level might serve as a useful biomarker for differentiating patients with CCC from those with HCs; the AUC was 0.77 (95% confidence interval, 0.65-0.89) and the sensitivity and specificity was 65 and 83%, respectively (Fig. 3).

We analyzed the relationship between serum miR-210 levels and clinicopathological parameters. There was no significant association between serum miR-210 levels and age, sex, tumor size, or existence of metastasis at diagnosis (Fig. 4). Although serum miR-210 level tended to be higher in patients with metastasis at diagnosis when compared with patients without metastasis (P=0.067; Fig. 4D), this difference did not reach the level of statistical significance.

Discussion

Previous studies have described the potential use of circulating microRNA as a non-invasive biomarker for various cancers [e.g., miR-29a and miR-92 in colorectal cancer (9); miR-195 in breast cancer (14); miR-17-5p, miR-21, miR-106a and miR-106b in gastric cancer (15); and miR-141 and miR-26a in prostate cancer (6,16)]. In the case of RCC, several recent

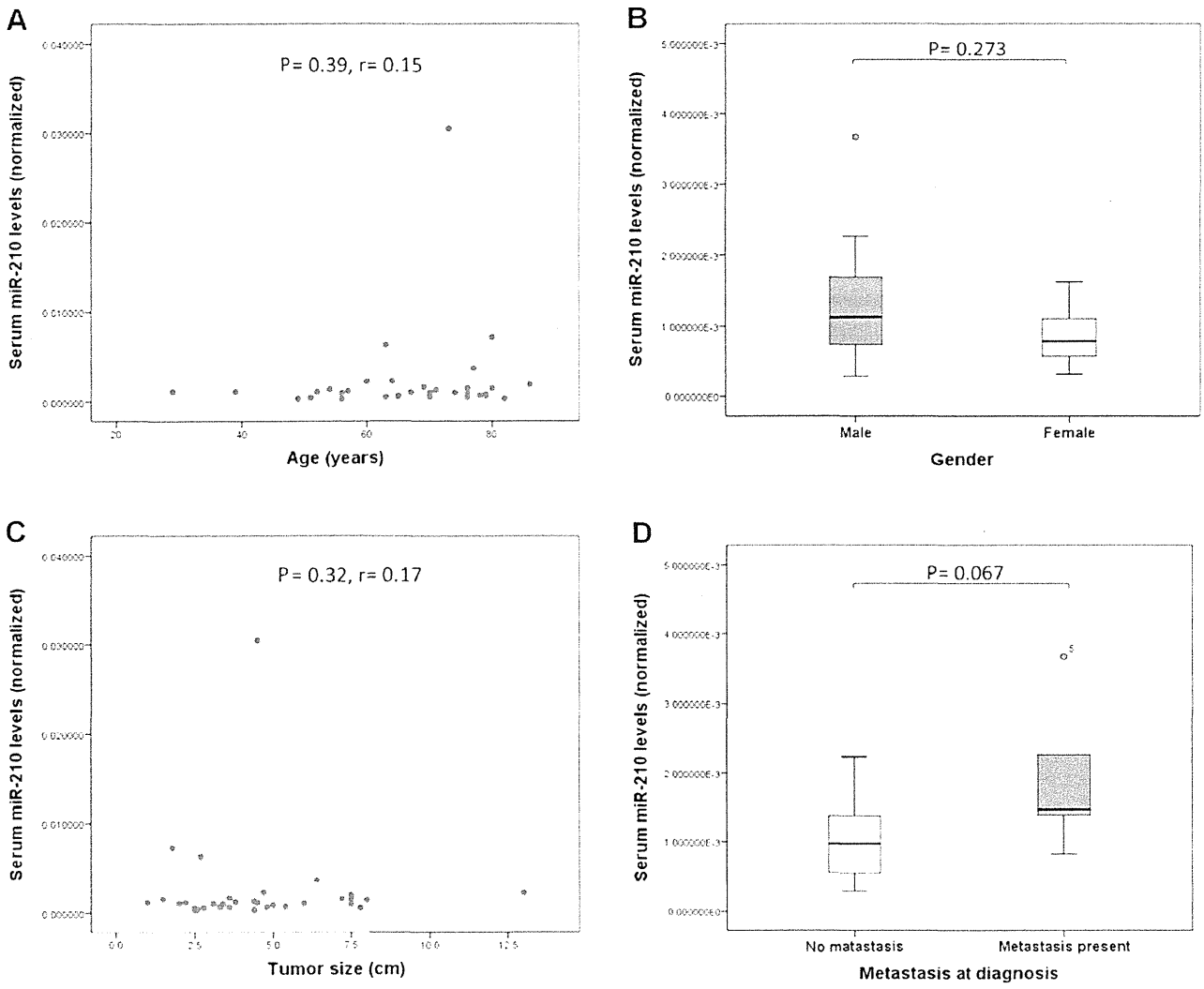

Figure 4. Analysis of the correlation between serum miR-210 levels and clinicopathological parameters. There was no significant association between serum miR-210 levels and age (A), gender (B), tumor size (C), or existence of metastasis at diagnosis (D).

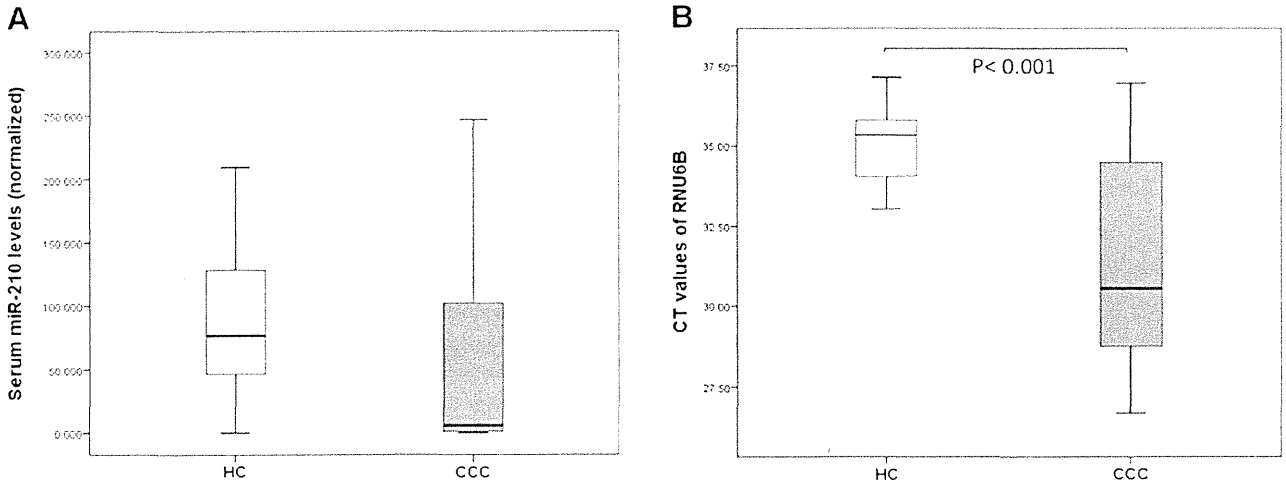

Figure 5. (A) There were no significant differences in serum miR-210 levels normalized against RNU6B when comparing 34 CCC patients and 23 HCs. (B) CT values of miR-16 in 34 CCC patients and in 23 HCs. CT values of RNU6B were significantly lower in CCC patients than in HCs (P<0.001). Moreover, there was marked variability of the Ct values when comparing CCC patients and HCs.

studies using miRNA microarray analysis showed different microRNA expression profiles when comparing tumor tissues and matched normal tissues. However, some of the data regarding the number and type of up-/downregulated microRNAs is conflicting (17-19). Regardless, several recent studies have described the use of circulating microRNA as a new biomarker for RCC.

The present study showed that serum miR-210 levels were significantly higher in CCC patients than in HCs. Furthermore, there was no correlation between serum miR-210 levels and clinicopathological parameters. These results indicate that upregulation of serum miR-210 may occur in the early stage of CCC and can serve as a potential biomarker of early diagnosis in CCC.

Four studies have investigated the utility of circulating microRNAs as a diagnostic biomarker for RCC. Wulfken *et al* were the first to report that the serum miR-1233 level was increased in 84 patients with RCC from a multicenter cohort (AUC, 0.588; sensitivity, 77.4%; specificity, 37.6%). Moreover, they investigated 13 samples from patients with angiomyolipoma or oncocytoma whose serum miR-1233 levels were similar to those of patients with RCC (20). Redova *et al* also demonstrated that serum miR-378 and miR-451 were potential biomarkers for RCC. When the utility of miR-378 and miR-451 was evaluated in an independent cohort of 90 patients with RCC and 35 HCs, the combination of serum miR-378 and miR-451 enabled identification of RCC with relatively high accuracy rate (AUC 0.86; sensitivity, 81%; specificity, 83%) (21). Hauser *et al* confirmed that serum miR-378 was significantly increased in 25 CCC patients (P=0.006), but they did not detect a difference in the level of this biomarker when comparing 117 patients with RCC versus 123 HCs (22). Zhao *et al* reported that tissue miR-210 levels in 33 CCC patients were significantly higher in tumor tissue than in adjacent non-tumoral renal parenchyma (P=0.004). Serum miR-210 levels were also significantly higher in 68 CCC patients than in 42 HCs (P<0.001) (AUC, 0.87; sensitivity, 81.0%; specificity, 79.4%). Furthermore, serum miR-210 levels in patients with CCC decreased by 1 week after surgical resection of the tumor (23).

The present study normalized the assessed RNA values in tissue and serum against those of miR-145 and miR-16, respectively, which is a different approach from that used by Zhao *et al*. There is no consensus regarding the optimal normalization gene to use for quantitative real-time polymerase chain reaction (qRT-PCR) analysis of circulating mRNAs (24). The present study did not utilize RNU6B or 5s rRNA for normalization of qRT-PCR data because some studies have reported that RNU6B and 5s rRNA were not stable in human tissues or body fluids. In their study targeting serum miRNA in gastric cancer patients, Song *et al* demonstrated that RNU6B could not be detected in almost half of the serum samples; in the other half of patients, it was detected with Ct values of >40. Moreover, RNU6B was less stably expressed than let-7a and miR-16 in normal and cancerous human solid tissues (25). Although we actually examined the same study using RNU6B for normalization, there was marked variation in Ct values when comparing CCC patients and HCs (Fig. 5). Therefore, we selected other miRNAs (miR-16, miR-103a, miR-122 and miR-145) for the purposes of normalization, based on previous reports (21,26). Then, we determined which of these miRNAs was expressed in similar amounts when comparing CCC patients and HCs. As a result of these investigations, miR-145 and miR-16 were selected for use as normalizing genes in the present study.

MiR-210 is upregulated in various types of human cancers, suggesting its important role in tumorigenesis (27). Jung *et al* reported that plasma miR-210 levels in human breast cancer were associated with trastuzumab sensitivity, tumor presence and lymph node metastasis (28). Although the mechanism of upregulation of miR-210 is still unclear, some groups have reported that miR-210 is induced under-hypoxic conditions via hypoxia-inducible factors (HIFs) in various cancer cell lines (28). It is well known that HIF1α and HIF2α accumulate in CCC as a result of abrogated ubiquitin-mediated degradation due to loss or deficiency of the *von Hippel-Lindau tumor suppressor (VHL)* tumor suppressor gene (29). Nakada *et al* demonstrated that miR-210 was highly expressed in RCC cell lines and that its expression clearly correlated with the accumulation of hypoxia-inducible factor 1α (HIF1α) under normoxia as well as under hypoxia, suggesting that miR-210 upregulation in CCC was most likely due to accumulation of HIF1α. Further, they confirmed that restoration of VHL expression in the VHL-deficient cell line led to the degradation of HIF1α and suppressed the expression of miR-210, suggesting that miR-210 expression is regulated via the VHL-HIF1α pathway (11). Since VHL inactivation is observed in >70% of CCC patients, its inactivation may occur in the early stage of tumorigenesis. This raises the possibility that the expression of miR-210 is upregulated and plays a role in the early stage of tumorigenesis in CCC tissue and that serum miR-210 is upregulated in the human peripheral blood in the early stages of CCC.

For these reasons, serum miR-210, which can be easily measured on an outpatient basis, could be a useful biomarker for early diagnosis and facilitate earlier treatment and, hence, improves outcomes. Further studies with a larger number of patients are warranted to validate these results.

In conclusion, early detection and treatment of RCC is critical to improve outcomes. Serum miR-210 is a useful biomarker for early CCC.

References

1. Hollingsworth JM, Miller DC, Daignault S and Hollenbeck BK: Rising incidence of small renal masses: a need to reassess treatment effect. J Natl Cancer Inst 98: 1331-1334, 2006.
2. Devita VT Jr, Hellman S and Rosenberg SA: Cancer Principles and Practice of Oncology. 8th edition, Lippincott Williams & Wilkins, 2008.
3. Ljungberg B, Cowan NC, Hanbury DC, Hora M, Kuczyk MA, Merseburger AS, Patard JJ, Mulders PF, Sinescu IC; European Association of Urology Guideline Group: EAU guidelines on renal cell carcinoma: the 2010 update. Eur Urol 58: 398-406, 2010.
4. Slaby O, Jancovicova J, Lakomy R, Svoboda M, Poprach A, Fabian P, Kren L, Michalek J and Vyzula R: Expression of miRNA-106b in conventional renal cell carcinoma is a potential marker for prediction of early metastasis after nephrectomy. J Exp Clin Cancer Res 29: 90, 2010.
5. Volinia S, Calin GA, Liu CG, Ambs S, Cimmino A, Petrocca F, Visone R, Iorio M, Roldo C, Ferracin M, Prueitt RL, Yanaihara N, Lanza G, Scarpa A, Vecchione A, Negrini M, Harris CC and Croce CM: A microRNA expression signature of human solid tumors defines cancer gene targets. Proc Natl Acad Sci USA 103: 2257-2261, 2006.

6. Mitchell PS, Parkin RK, Kroh EM, Fritz BR, Wyman SK, Pogosova-Agadjanyan EL, Peterson A, Noteboom J, O'Briant KC, Allen A, Lin DW, Urban N, Drescher CW, Knudsen BS, Stirewalt DL, Gentleman R, Vessella RL, Nelson PS, Martin DB and Tewari M: Circulating microRNAs as stable blood-based markers for cancer detection. Proc Natl Acad Sci USA 105: 10513-10518, 2008.
7. Chim SS, Shing TK, Hung EC, Leung TY, Lau TK, Chiu RW and Lo YM: Detection and characterization of placental microRNAs in maternal plasma. Clin Chem 54: 482-490, 2008.
8. Hunter MP, Ismail N, Zhang X, Aguda BD, Lee EJ, Yu L, Xiao T, Schafer J, Lee ML, Schmittgen TD, Nana-Sinkam SP, Jarjoura D and Marsh CB: Detection of microRNA expression in human peripheral blood microvesicles. PLoS One 3: e3694, 2008.
9. Huang Z, Huang D, Ni S, Peng Z, Sheng W and Du X: Plasma microRNAs are promising novel biomarkers for early detection of colorectal cancer. Int J Cancer 127: 118-126, 2010.
10. Roth C, Rack B, Müller V, Janni W, Pantel K and Schwarzenbach H: Circulating microRNAs as blood-based markers for patients with primary and metastatic breast cancer. Breast Cancer Res 12: R90, 2010.
11. Nakada C, Tsukamoto Y, Matsuura K, Nguyen TL, Hijiya N, Uchida T, Sato F, Mimata H, Seto M and Moriyama M: Overexpression of miR-210, a downstream target of HIF1α, causes centrosome amplification in renal carcinoma cells. J Pathol 224: 280-288, 2011.
12. Crosby ME, Kulshreshtha R, Ivan M and Glazer PM: MicroRNA regulation of DNA repair gene expression in hypoxic stress. Cancer Res 69: 1221-1229, 2009.
13. Fasanaro P, D'Alessandra Y, Di Stefano V, Melchionna R, Romani S, Pompilio G, Capogrossi MC and Martelli F: MicroRNA-210 modulates endothelial cell response to hypoxia and inhibits the receptor tyrosine kinase ligand Ephrin-A3. J Biol Chem 283: 15878-15883, 2008.
14. Heneghan HM, Miller N, Lowery AJ, Sweeney KJ, Newell J and Kerin MJ: Circulating microRNAs as novel minimally invasive biomarkers for breast cancer. Ann Surg 251: 499-505, 2010.
15. Tsujiura M, Ichikawa D, Komatsu S, Shiozaki A, Takeshita H, Kosuga T, Konishi H, Morimura R, Deguchi K, Fujiwara H, Okamoto K and Otsuji E: Circulating microRNAs in plasma of patients with gastric cancers. Br J Cancer 102: 1174-1179, 2010.
16. Mahn R, Heukamp LC, Rogenhofer S, von Ruecker A, Müller SC and Ellinger J: Circulating microRNAs (miRNA) in serum of patients with prostate cancer. Urology 77: 1265.e9-16, 2011.
17. Redova M, Svoboda M and Slaby O: MicroRNAs and their target gene networks in renal cell carcinoma. Biochem Biophys Res Commun 405: 153-156, 2011.
18. White NM, Bao TT, Grigull J, Youssef YM, Girgis A, Diamandis M, Fatoohi E, Metias M, Honey RJ, Stewart R, Pace KT, Bjarnason GA and Yousef GM: miRNA profiling for clear cell renal cell carcinoma: biomarker discovery and identification of potential controls and consequences of miRNA dysregulation. J Urol 186: 1077-1083, 2011.
19. Wotschofsky Z, Busch J, Jung M, Kempkensteffen C, Weikert S, Schaser KD, Melcher I, Kilic E, Miller K, Kristiansen G, Erbersdobler A and Jung K: Diagnostic and prognostic potential of differentially expressed miRNAs between metastatic and non-metastatic renal cell carcinoma at the time of nephrectomy. Clin Chim Acta 416: 5-10, 2013.
20. Wulfken LM, Moritz R, Ohlmann C, Holdenrieder S, Jung V, Becker F, Herrmann E, Walgenbach-Brünagel G, von Ruecker A, Müller SC and Ellinger J: MicroRNAs in renal cell carcinoma: diagnostic implications of serum miR-1233 levels. PLoS One 6: e25787, 2011.
21. Redova M, Poprach A, Nekvindova J, Iliev R, Radova L, Lakomy R, Svoboda M, Vyzula R and Slaby O: Circulating miR-378 and miR-451 in serum are potential biomarkers for renal cell carcinoma. J Transl Med 10: 55, 2012.
22. Hauser S, Wulfken LM, Holdenrieder S, Moritz R, Ohlmann CH, Jung V, Becker F, Herrmann E, Walgenbach-Brünagel G, von Ruecker A, Müller SC and Ellinger J: Analysis of serum microRNAs (miR-26a-2*, miR-191, miR-337-3p and miR-378) as potential biomarkers in renal cell carcinoma. Cancer Epidemiol 36: 391-394, 2012.
23. Zhao A, Li G, Péoc'h M, Genin C and Gigante M: Serum miR-210 as a novel biomarker for molecular diagnosis of clear cell renal cell carcinoma. Exp Mol Pathol 94: 115-120, 2013.
24. Kroh EM, Parkin RK, Mitchell PS and Tewari M: Analysis of circulating microRNA biomarkers in plasma and serum using quantitative reverse transcription-PCR (qRT-PCR). Methods 50: 298-301, 2010.
25. Song J, Bai Z, Han W, Zhang J, Meng H, Bi J, Ma X, Han S and Zhang Z: Identification of suitable reference genes for qPCR analysis of serum microRNA in gastric cancer patients. Dig Dis Sci 57: 897-904, 2012.
26. Cheng Y, Wang X, Yang J, Duan X, Yao Y, Shi X, Chen Z, Fan Z, Liu X, Qin S, Tang X and Zhang C: A translational study of urine miRNAs in acute myocardial infarction. J Mol Cell Cardiol 53: 668-676, 2012.
27. Camps C, Buffa FM, Colella S, Moore J, Sotiriou C, Sheldon H, Harris AL, Gleadle JM and Ragoussis J: hsa-miR-210 is induced by hypoxia and is an independent prognostic factor in breast cancer. Clin Cancer Res 14: 1340-1348, 2008.
28. Jung EJ, Santarpia L, Kim J, Esteva FJ, Moretti E, Buzdar AU, Di Leo A, Le XF, Bast RC Jr, Park ST, Pusztai L and Calin GA: Plasma microRNA 210 levels correlate with sensitivity to trastuzumab and tumor presence in breast cancer patients. Cancer 118: 2603-2614, 2012.
29. Eble JN, Sauter G, Epstein JI and Sesterhenn IA (eds.): World Health Organization Classification of Tumours. Pathology and Genetics of Tumours of the Urinary System and Male Genital Organs. IARC Press, Lyon, pp9-87, 2004.